Deciphering regulation of FOXP3 expression in human conventional T cells

Jennifer M. Umhoefer[1,2,3], Maya M. Arce[1,2,3], Rama Dajani[1], Julia A. Belk[4], Cody T. Mowery[1,2,3], Vinh Nguyen[1,2,5,6,7], Benjamin G. Gowen[8,9], Dimitre R. Simeonov[2,3], Gemma L. Curie[8,9], Jacob E. Corn[10], Howard Y. Chang[4,11], Alexander Marson[1,2,8,12,13,14,15,§]

[1] Gladstone-UCSF Institute of Genomic Immunology, San Francisco, CA, USA.
[2] Department of Medicine, University of California, San Francisco, CA, USA.
[3] Biomedical Sciences graduate program, University of California, San Francisco, CA, USA
[4] Center for Personal Dynamic Regulomes, Stanford University School of Medicine, Stanford, CA, USA.
[5] Diabetes Center, University of California, San Francisco, San Francisco, CA, USA.
[6] Department of Surgery, University of California, San Francisco, San Francisco, CA, USA.
[7] UCSF CoLabs, University of California, San Francisco, San Francisco, CA, USA.
[8] Innovative Genomics Institute, University of California, Berkeley, Berkeley, CA, USA.
[9] Department of Molecular and Cell Biology, University of California, Berkeley, Berkeley, CA, USA.
[10] Department of Biology, Institute of Molecular Health Sciences, ETH Zürich, Switzerland.
[11] Howard Hughes Medical Institute, Stanford University, Stanford, CA, USA.
[12] Department of Laboratory Medicine, University of California, San Francisco, CA, USA.
[13] UCSF Helen Diller Family Comprehensive Cancer Center, University of California, San Francisco, CA, USA.
[14] Department of Microbiology and Immunology, University of California, San Francisco, CA, USA.
[15] Institute for Human Genetics, University of California, San Francisco, CA, USA.
[§] e-mail: alex.marson@gladstone.ucsf.edu

ABSTRACT

FOXP3 is a lineage-defining transcription factor that controls differentiation and maintenance of suppressive function of regulatory T cells (Tregs). Foxp3 is exclusively expressed in Tregs in mice. However, in humans, FOXP3 is not only constitutively expressed in Tregs; it is also transiently expressed in stimulated CD4+CD25- conventional T cells (Tconvs)[1–3]. Mechanisms governing the expression of FOXP3 in human Tconvs are not understood. Here, we performed CRISPR interference (CRISPRi) screens using a 15K-member gRNA library tiling 39 kb downstream of the *FOXP3* transcriptional start site (TSS) to 85 kb upstream of the TSS in Treg and Tconvs. The *FOXP3* promoter and conserved non-coding sequences (CNS0, CNS1, CNS2 and CNS3), characterized as enhancer elements in murine Tregs, were required for maintenance of FOXP3 in human Tregs. In contrast, FOXP3 in human Tconvs depended on regulation at CNS0 and a novel Tconv-specific noncoding sequence (TcNS+) located upstream of CNS0. Arrayed validations of these sites identified an additional repressive cis-element overlapping with the *PPP1R3F* promoter (TcNS-). Pooled CRISPR knockouts revealed multiple transcription factors required for proper expression of FOXP3 in Tconvs, including GATA3, STAT5, IRF4, ETS1 and DNA methylation-associated regulators DNMT1 and MBD2. Analysis of ChIP-seq and ATAC-seq paired with knock-out (KO) of GATA3, STAT5, IRF4, and ETS1 revealed regulation of CNS0 and TcNS+ accessibility. Collectively, this work identified Treg-shared and Tconv-specific cis-elements and the trans-factors that interact with them, building a network of regulators controlling FOXP3 expression in human Tconvs.

Background

Regulatory T cells (Tregs) are a specialized subset of CD4+ T cells that maintain self-tolerance and immune homeostasis. The transcription factor FOXP3 is a lineage-defining factor in Tregs, and its continued expression is crucial for proper Treg differentiation, suppressive function, and maintenance of cellular identity. In mice, expression of Foxp3 is exclusive to Tregs, and FOXP3 therefore serves as a useful marker for Treg identification[4,5]. However, Treg-specific expression of FOXP3 is not conserved in human cells. Both human Tregs and CD4+CD25- conventional T cells (Tconvs) are capable of FOXP3 expression, with the former exhibiting constitutive expression and the latter transient expression upon cellular activation[1–3]. In vitro stimulation via CD3 is sufficient to induce FOXP3 expression in a subset of Tconvs, and combination with CD28 stimulation and/or exogenous IL-2 further enhances the proportion of FOXP3+ Tconvs in vitro[1,2]. Strong in vitro activation signals are capable of inducing FOXP3 expression in almost all Tconvs[1,2]. While the function of FOXP3 is well-characterized in Tregs, the functional significance of FOXP3 expression in human Tconvs is not fully understood. Transient expression of FOXP3 does not prevent proliferation or expression of pro-inflammatory cytokines, including IL-2 and INF-γ[2,3]. FOXP3 expression in Tconvs has been shown to decrease sensitivity to restimulation-induced cell death[6], indicating a potential role in modulating activation responses.

Similarly, regulators of FOXP3 expression in human and murine Tregs have been extensively deciphered, while those governing expression in Tconvs remain largely unknown. In Tregs, four evolutionarily conserved noncoding sequences with FOXP3 enhancer activity, named CNS0-3, have been identified in the *FOXP3* locus. These cis-regulatory sequences regulate distinct aspects of FOXP3 expression. CNS0, which lies upstream of the *FOXP3* promoter, is involved in IL-2 induced FOXP3 expression during thymic Treg development[7,8]. CNS1 and CNS2 lie within intron 1 of *FOXP3*. CNS1 deficiency in mice is associated with impaired peripheral induction of

Foxp3 in gut-associated lymphoid tissue, mesenteric lymph nodes, and during differentiation of induced Tregs (iTregs) from naïve CD4+ T cells[9]. CNS2 controls heritable maintenance of FOXP3, and its stable activity is dependent on demethylation of CpG dinucleotides within the element[9,10]. Finally, CNS3 lies within intron 2 of *FOXP3* and regulates de novo induction of FOXP3 expression in thymic and peripheral Treg development[9]. Trans-acting transcription factors and chromatin modifiers that interact with these cis-elements have also been characterized, including, for example, STAT5 at CNS0, NFAT and Smad3 at CNS1, Foxp3, Runx1, Cbf-β, and GATA3 at CNS2, and c-Rel at CNS3[7–9,11–13]. More recent CRISPR nuclease (CRISPRn) screens, mostly in murine Tregs, have identified additional transcription factors, chromatin modifiers, and post-transcriptional factors that integrate into gene regulatory circuits controlling Foxp3 expression [14–16].

DNA is differentially regulated in the *FOXP3* locus between Tregs and Tconvs. In both human and murine systems, CNS2 is demethylated in Tregs but near-completely methylated in Tconvs, including naïve CD4+ T cells that are capable of differentiation into iTregs[9,10,17]. Tregs and Tconvs additionally have differential methylation at the *FOXP3* promoter, with demethylation in Tregs and partial methylation in Tconvs[10,18]. Furthermore, inhibition of the maintenance DNA methyltransferase DNMT1, which maintains methylation status, induces FOXP3 expression in Tconvs, further indicating a role for DNA methylation in the regulation of FOXP3 expression in Tconvs[19].

To discover cis- and trans-regulators of FOXP3 expression in human Tconvs, we performed CRISPR interference (CRISPRi) screens tiling the *FOXP3* locus in Treg and Tconvs and CRISPRn screens targeting trans-acting regulators in Tconvs. We previously used CRISPRi tiling screens to identify cis-regulatory regions within the *CD28-CTLA4-ICOS* locus[20]. Here, using CRISPRi tiling screens surrounding *FOXP3*, we identified Tconv enhancers of *FOXP3* expression at CNS0 and a novel Tconv-specific noncoding sequence (TcNS+) located upstream of CNS0. Arrayed validations of these sites additionally identified a suppressive cis-element overlapping with the *PPP1R3F* promoter (TcNS-). In parallel, CRISPRn trans-regulator screening identified multiple trans-factors, including GATA3, STAT5, IRF4, ETS1 and DNA methylation-associated regulators DNMT1 and MBD2. Analysis of ChIP-seq and ATAC-seq paired with knock-out (KO) of GATA3, STAT5, IRF4, and ETS1 revealed regulation of CNS0 and TcNS+ accessibility. Collectively, this work identified Tconv cis-elements and the trans-factors that interact with them, building a network of regulators controlling FOXP3 expression in human Tconvs.

Results

CRISPRi tiling screen identifies cis-elements controlling FOXP3 expression

To map FOXP3 cis-regulatory regions systematically, we designed a pooled CRISPRi screen targeting the *FOXP3* locus (Figure 1A). The gRNA library consisted of 15K gRNA spanning a ~123 kb region from 39 kb downstream of the *FOXP3* transcriptional start site (TSS) to 85 kb upstream of the TSS. We isolated CD4+CD25^{low} human Tconvs and CD4+CD25^{high}CD127^{low} human Tregs from the blood of two healthy donors and stimulated cells with anti-CD3/CD28 beads. One and two days post-stimulation, we lentivirally delivered dCas9-ZIM3 CRISPRi machinery followed by the gRNA library. Infected cells were selected using puromycin, expanded, and high cell purity of HELIOS+FOXP3+ Treg cultures and HELIOS-FOXP3- Tconv

cultures was verified (Figure S1A). Cells were restimulated on day 9 post-initial stimulation. Forty-eight hours post restimulation, when Tconvs express elevated levels of FOXP3 (Figure S1B), cells were fixed/permeabilized and stained for FOXP3 expression, and FACS-sorted into bins of high (top ~25%) and low (bottom ~25%) FOXP3 expression (Figure S1C).

We identified cis-regulatory elements involved in both maintenance and repression of FOXP3 expression (Figure 1B). Consistency was observed between Treg and Tconv donors (Figure S1D). As expected, the TSS of *FOXP3* was the most responsive to CRISPRi tiling in both Tconv and Treg, resulting in significant gRNA enrichment in the FOXP3 low bin, indicating the strongest role in FOXP3 maintenance within the locus. In human Tregs, numerous gRNAs across the first 8 kb of the *FOXP3* gene body showed similar responsiveness to CRISPRi. Significant gRNAs enriched in the FOXP3 low bin mapped to CNS1, 2, and 3. However, no significant gRNAs in these regions were enriched in the FOXP3 low Tconv bin, suggesting that these enhancers are not essential for FOXP3 induction in Tconvs (Figure 1B). We also identified a Treg-specific 4.6 kb FOXP3-repressive element 1.1 kb upstream of the *FOXP3* TSS that maps to *FLICR*, a lncRNA transcript described in mice[21]. Previous work has shown that *Flicr* is specifically expressed in Tregs and acts in cis to negatively regulate *Foxp3* expression[21]. Interestingly, we identified cis-elements controlling FOXP3 induction in Tconvs, one of which was distinct from the elements required for FOXP3 maintenance in Tregs (Figure 1B). CNS0 was critical for FOXP3 expression in both human Treg and Tconvs (Figure 1B). A 2 kb non-conserved non-coding sequence (TcNS+) approximately 11.8 kb upstream of the *FOXP3* TSS emerged as a selective Tconv-specific regulator of FOXP3 induction (Figure 1B). Analysis of ATAC-seq in stimulated and unstimulated Tregs and Tconvs[22] revealed CNS0 and TcNS+ increase accessibility upon stimulation (Figure S1E), which mirrors Tconv FOXP3 induction upon stimulation. Taken together, our CRISPRi screens revealed that FOXP3 expression in human Tconvs depends on a set of cis-regulatory elements distinct from the well-characterized Treg elements and nominated a novel element selectively required in Tconvs.

To validate the results of the CRISPRi screens and assess the quantitative effects of cis-element perturbation on FOXP3 expression, we designed an orthogonal CRISPRn deletion strategy using paired Cas9 RNPs to excise elements of interest. Using this strategy, we designed Cas9 RNPs to generate 24 different ~1 kb deletions across the *FOXP3* TSS, *FLICR*, CNS0, and TcNS+ in resting and stimulated human Tregs and Tconvs. In an arrayed fashion, we measured FOXP3 MFI (Tregs; Figure 1C) and the percent of FOXP3+ cells (Tconvs; Figure 1D) for each targeted deletion and for AAVS1-targeted control cells.

Treg tiled deletions revealed a rapid transition from FOXP3-maintenance cis-elements (Tiles 1-5, Figure 1C) to suppressive elements (Tiles 6-9, Figure 1C), particularly at 0 hours post-stimulation. Deletions targeting the TSS (Tile 4) and CNS0 (Tiles 18-21) decreased FOXP3 in both Tregs and Tconvs, with the largest CNS0 effect observed at Tile 21 in Tregs and 18 in Tconvs. Deletion of one tile of TcNS+ in Tconvs led to a decreased percentage of FOXP3+ cells in resting Tconvs and a mild decrease in activated Tconvs (Tile 23). Interestingly, in resting Tconvs, which differed from the stimulation state used in the screen, deletion of tiles overlapping with the promoter and TSS of the neighboring gene *PPP1R3F* resulted in a large increase in the percent of FOXP3+ Tconvs, while KO of PPP1R3F did not increase FOXP3 expression in resting or stimulated Tconvs or Tregs (Figure 1D-F). These results indicate that CRISPRi-

responsive CNS0 and TcNS+ positively regulate FOXP3 expression in Tconvs, while the *PPP1R3F* promoter region (TcNS-), which has the strongest effect in resting Tconvs, negatively regulates FOXP3 expression in Tconvs.

Defining critical trans-regulators of Tconv FOXP3 expression with CRISPR KO screens

To identify trans-regulators required for FOXP3 expression in human Tconvs, we performed a pooled SLICE-based CRISPRn genetic screen in primary human Tconvs (Figure 2A)[23]. We used a library of 6000 gRNAs targeting 1349 human transcription factors, chromatin modifiers, and immune genes in addition to non-targeting controls[24]. We isolated CD4+CD25^{low} human Tconvs from the blood of three healthy donors, stimulated cells with anti-CD3/CD28 beads, and delivered the gRNA library via lentivirus and Cas9 ribonucleoproteins (RNPs) via electroporation. Cells were expanded and restimulated on day 9 post-initial stimulation. Two-days post restimulation, cells were fixed and stained for FOXP3 expression, and sorted via FACS into bins of high (top ~25%) and low (bottom ~25%) FOXP3 expression (Figure 2A, Figure S2A).

We achieved sufficient cellular coverage (Figure S2B) to identify 23 positive regulators and 15 negative regulators of FOXP3 expression in human Tconvs (FDR ≤ 0.05; Figure 2B). Multiple individual gRNAs targeting significant gene regulators were consistently enriched in FOXP3 high or low FACS bins for repressor or maintenance genes, respectively, and consistency in gene hits was observed between individual donors (Figure 2C, Figure S2C-E). Multiple positive regulators of Tconv FOXP3 expression have previously been linked to FOXP3 expression in mouse and/or human Tregs, including GATA3[13], STAT5A/STAT5B[7,25], and ATXN7L3[14]. However, until now these regulators have not been shown to influence FOXP3 expression in human Tconvs.

We next validated the effects of individual transcription factor KOs in arrayed fashion. For top candidate transcription factors that promoted or repressed FOXP3 in the pooled screen, we performed arrayed KO and measured the percentage of FOXP3+ cells and FOXP3 levels in resting and stimulated (48 hours post-stimulation) Tconvs via flow cytometry (Figure 2D-E, S3A-C). We achieved high editing efficiency of KOs as assessed by targeted amplicon sequencing (mean percentage modified reads of 92.0%; Figure S3D). Nearly all individual KOs replicated the directionality of FOXP3 changes observed in the pooled screen (Figure 2D). GATA3 KO and FOXO1 KO both resulted in large reductions in the percentage of FOXP3+ cells at 48 hours post-stimulation, decreasing the percentage of FOXP3+ cells nearly to levels of FOXP3 KO (Figure 2D-E). BCL11B KO also yielded a large reduction in the percentage of FOXP3+ cells. FOXP3 is minimally expressed in resting Tconvs, enabling more sensitive identification of regulator KOs that increased FOXP3 expression in resting cells. KO of TFDP1, ETS1, and DNMT1 resulted in the largest increase in FOXP3 expression in resting Tconvs, with DNMT1 KO increasing the percentage FOXP3+ cells 14.9-fold relative to AAVS1 controls (Figure 2D). At 48 hours post-stimulation, DNMT1, TFDP1, and ETS1 KOs also increased the percentage FOXP3+ cells, along with KOs of YBX1 and methyl-CpG binding domain protein MBD2 (Figure 2D-E), although DNMT1 KO resulted in high cell toxicity post-stimulation. The observed repression of FOXP3 in Tconvs by DNMT1 (a maintenance DNA methyl transferase) and MBD2 is consistent with previous studies describing the importance of methylation at the

FOXP3 locus (including at the promoter and CNS2) limiting FOXP3 expression in Tconvs[9,10,17–19].

A distinct and only partially overlapping set of Tconv regulators also displayed FOXP3 regulation in Tregs, including, most prominently, positive regulators GATA3 and FOXP1 and negative regulators DNMT1, TFDP1, YBX1, and ETS1 (48 hrs. post-stimulation, Figure S3E). BCL11B KO showed no effect on FOXP3 expression at either timepoint, despite strong effects on the %FOXP3+ cells in Tconvs (Figure 2D, Figure S3E). Collectively, arrayed perturbation distinguished Tconv trans-regulators of FOXP3 expression, highlighting FOXO1, GATA3, and STAT5 as top positive regulators, and ETS1 and DNA methylation-associated regulators DNMT1 and MBD2 as top repressors of FOXP3 expression in Tconvs.

Trans-regulators bind to TcNS-, CNS0, and TcNS+ to control FOXP3 expression

We next attempted to integrate trans-regulators and FOXP3 cis-regulatory elements into networks controlling expression of FOXP3 in human Tconvs. To understand how trans-regulators affect expression in the broader *FOXP3* locus and of each other, we assessed differential expression of genes within the CRISPRi-tiled *FOXP3* locus and of FOXP3 trans-regulators using published KO RNA-seq datasets from our group[24]. KO RNA-seq datasets were available for 9 regulators in human Tconvs, including ATXN7L3, ETS1, FOXP1, GATA3, IRF2, IRF4, MBD2, STAT5A, and YY1, and changes in expression were compared to AAVS1-targeted controls. At the *FOXP3* locus, KO of positive regulators STAT5B and GATA3 decrease expression of PPP1R3F in addition to FOXP3, while KO of negative regulator ETS1 increases PPP1R3F and FOXP3 expression (Figure S4A), indicating FOXP3 trans-regulators contribute to regulation of genes surrounding the *FOXP3* locus. Interestingly, KO of multiple positive regulators decrease STAT5B and ZBTB32 levels (Figure S4B), indicating regulators may converge on STAT5B and ZBTB32, or pathways that induce their expression.

Motif analysis using predicted transcription factor motifs from CisBP[26] and JASPAR[27] highlighted candidate binding sequences of trans-regulators at the *FOXP3* locus. Binding motifs for positive *FOXP3* trans-regulators were present across the *FOXP3* locus, including at the *FOXP3* TSS (YY1, FOXO1, FOXP1, IRF4, GATA3, IKZF3, and STAT5A), at CNS0 (YY1, IKZF1, IRF4, GATA3, NFKB2, and BCL11B), and at the novel Tconv-specific TcNS+ (YY1, FOXO1, FOXP1, BCL11B, STAT5A, and STAT5B, among others; Figure 3A). Interestingly, binding motifs for positive FOXP3 regulator YY1, which is associated with maintenance of enhancer-promoter loops and activating and repressive chromatin modifiers[28,29], and ZBTB32, a positive regulator with reported chromatin-repressive activity[30,31], aligned in or proximal to TcNS- (Figure 3A). Binding motifs for numerous negative FOXP3 trans-regulators nominated by our transcription factor screens in Tconvs clustered within TcNS-, including motifs for EGR2, ETS1, DNMT1, TFDP1, and MBD2, among others (Figure 3A).

We next analyzed regulators with available ChIP-seq datasets in T cells and T cell lines to assess overlap with FOXP3 cis-elements. Positive regulators BCL11B, GATA3, and STAT5B bound CNS0, with additional BCL11B and YY1 binding at TcNS- and STAT5B binding at TcNS+ (Figure 3B). Few ChIP-seq datasets targeting negative regulators were available, so we analyzed datasets generated in other hematopoietic cells and hematopoietic cell lines, which indicated MBD2 and TFDP1 binding at TcNS- (Figure 3C). In short, motif and ChIP-seq analysis suggests

that multiple factors promoting FOXP3 expression in human Tregs may bind directly to CNS0 and TcNS+, two enhancers critical for expression of FOXP3 in human Tconvs. Binding of multiple factors to TcNS- could conversely limit FOXP3 levels in human Tconvs.

We next assessed the effect of FOXP3 regulators on chromatin state at *cis*-regulatory regions required for proper FOXP3 expression. We used published datasets from our group complementary to KO RNA-seq datasets to measure changes in chromatin accessibility with KO of FOXP3 trans-regulators compared to AAVS1-targeted controls in CD4+CD25- Tconvs[24]. Among the nine regulators included in the KO ATAC-seq dataset, GATA3, IRF4, STAT5A, and ETS1 KO each resulted in differentially accessible peaks in the *FOXP3* locus (Figure 3D). KO of positive regulators GATA3, IRF4, and STAT5A caused decreased accessibility at CNS0 and TcNS+, and IRF4 KO additionally caused decreased accessibility at a distal accessible region within the *CACNA1F* gene body (Figure 3D). Decreased accessibility at TcNS+ with STAT5A KO is consistent with previous reports of a STAT5-responsive element in this region in murine Tregs[7]. GATA3 binding at CNS0, the site of a large change in accessibility, indicates GATA3 likely maintains FOXP3 expression in part via direct maintenance of CNS0 accessibility (Figure 3B, D). Similarly, STAT5B ChIP-seq in T cells treated with IL-2 aligned at both CNS0 and TcNS+, consistent with differential accessibility at these sites and indicative of a role of IL-2 signaling in CNS0 and TcNS+ function (Figure 3B, D). Collectively, numerous trans-regulators interact directly with FOXP3 cis-elements, including GATA3 and STAT5, which maintain accessibility at FOXP3 enhancer elements CNS0 and TcNS+.

Discussion

FOXP3 cis-regulatory elements and the transcription factors that bind them have been extensively characterized in Tregs, but regulation governing the transient expression of FOXP3 in human Tconvs has thus far remained elusive. This is in large part due to the absence of FOXP3 expression in murine Tconvs and because the majority of functional work has been performed in mouse models. Here, we perform *FOXP3* locus-tiling CRISPR screens and trans-regulator screens in primary human CD4+ T cells to identify cis- and trans-regulators controlling FOXP3 expression in Tconvs. We discovered that FOXP3 expression in Tconvs depends on both the CNS0 enhancer (which is also required in Tregs) and a Tconv-selective enhancer, TcNS+. On top of this, TcNS- was discovered as a critical repressor of FOXP3 expression in resting Tconvs. Subsets of CRISPR-nominated transcription factors that regulate FOXP3 levels in Tconvs were confirmed to directly bind to each of these elements.

Mirroring cis-regulators, trans-regulators of FOXP3 in Tconvs only partially overlap with Treg regulators. Non-overlapping regulators include Tconv-specific positive regulator BCL11B and repressor MBD2. In contrast, STAT5 and GATA3 strongly promote FOXP3 in both Tconvs and Tregs. In Tregs, their activity has been described at CNS2[13,25], which is methylated and inactive in Tconvs[9,10,17]. However, STAT5 additionally plays a critical role in Treg Foxp3 induction via CNS0[7,8] and binds the region associated with TcNS+ (previously described as a STAT5 responsive element in murine Tregs[7]), where its function has been unclear. Following our screens demonstrating the requirement of STAT5 and GATA3 for FOXP3 expression in Tconvs, we mined public data and found STAT5B also binds both CNS0 and TcNS+ in human Tconvs. Although interaction of GATA3 with Treg CNS0 has not been described, we found that GATA3 binds directly to CNS0 in Tconv subsets[32] and is required for proper CNS0 accessibility in

human Tconvs. Our tiling screens confirmed a strong reliance on CNS0 for FOXP3 expression in both human Tregs and Tconvs, suggesting that CNS0-binding factors, such as GATA3, may have a yet unappreciated role in FOXP3 expression in Tregs. More broadly, our work highlights potential mechanisms of FOXP3 expression that may be shared between maintenance of FOXP3 in Tregs and induction of FOXP3 in Tconvs while also nominating factors that operate selectively in Tconvs.

We identified key cis-regulators of FOXP3 expression in human Tconvs, including TcNS+ which is less well conserved among vertebrates than CNS0-3, which regulate FOXP3 in Tregs. However, precisely which cis-regulatory non-coding nucleotides have enabled the emergence of FOXP3 expression relative to murine Tconv remains unclear. CNS0 and portions of the TcNS- region overlapping with *PPP1R3F* exon 1 display relatively high conservation, but novel or altered motifs may exist in the less-conserved TcNS+ that could disrupt expression, upstream of the *PPP1R3F* TSS to strengthen silencing, or among other non-conserved non-coding sequences that were nonfunctional in our human screens but could exhibit suppression in mice. Nonetheless, our identification of a set of critical cis-regulatory sequences and trans-regulators provide a basis for functional and computational approaches to parse evolutionary changes that enable FOXP3 expression in human Tconvs, which does not occur in murine Tconvs.

Overall, this work characterized multiple novel cis-elements that enhance or limit FOXP3 expression in human Tconvs, identified transcription factors and chromatin modifiers that promote and repress FOXP3 expression, and characterized the role of select transcription factors in maintaining accessibility at FOXP3 enhancers. This work adds new complexity to regulation governing a gene indispensable to immune homeostasis by introducing novel cis-elements selectively active in Tconvs. This insight will inform ongoing efforts to enhance safety, stability, and efficacy of both Treg and Tconv-derived Treg cellular immunotherapies for treatment of autoimmune disease, transplant tolerance, and graft-versus-host-disease by introducing novel routes to manipulate in situ cis-elements to specifically enforce or silence FOXP3 expression.

Methods

Primary human T cell isolation and culture

Primary human T cells subsets were isolated from peripheral blood mononuclear cells (PBMCs) sourced from consented, fresh Human Peripheral Blood Leukopaks (STEMCELL Technologies, catalog no. 70500). Leukopaks were washed twice with 1X volume of EasySep Buffer (DPBS, 2% fetal bovine serum (FBS), 1 mM pH 8.0 EDTA) using centrifugation and resuspended at 150e6-200e6 cells/mL. CD4+CD25^{high}CD127^{low} Tregs and CD4+CD25^{low} Tconv were isolated from washed PBMCs using the EasySep Human CD4+CD127lowCD25+ Regulatory T Cell Isolation Kit (STEMCELL Technologies, catalog no. 18063) according to manufacturer's protocol. For enhanced cell purity, Tregs were stained for CD4 (Biolegend, catalog no. 344634 or 344620), CD25 (Tonbo, catalog no. 20-0259-T100), and CD127 (Becton Dickinson, catalog no. 557938) and further sorted into a CD4+CD25^{high}CD127^{low} population via FACS on a BD FACSAria or BD FACSAria Fusion I. Tregs and Tconvs were cultured in X-VIVO15 media (Lonza, catalog no. 02-053Q) supplemented with 5% FBS, 55 μM 2-Mercaptoethanol, and 4 mM N-Acetyl-L-Cysteine. For CRISPRi screening, CRISPRi validation, and CRISPRn screening, recombinant Human IL-2 (R&D Systems, catalog no. 202-GMP or BT-002-GMP) was supplemented at 200 IU/mL, and cells were stimulated for 48 hours with CTS Dynabeads

CD3/CD28 beads (Thermo Fisher Scientific, catalog no. 40203D) at a cell to bead ratio of 1:1. After 48 hours, beads were removed using magnetic separation. For all subsequent experiments, cells were cultured using recombinant Human IL-2 (R&D Systems, catalog no. 202-GMP or BT-002-GMP) supplemented at 300 IU/mL and stimulated with 12.5 uL/mL Immunocult Human CD3/CD28/CD2 T Cell Activator (STEMCELL Technologies, catalog no. 10970), to enhance cell recovery, growth, and viability. Cells were cultured at 37°C and 5% CO_2 and split to 5E5-1.5E6 cells/mL every 48 hours by topping off media and completely replacing the appropriate dose of IL-2.

Libraries and plasmids

The CRISPRi gRNA library was designed and cloned spanning approximately chrX:49,225,440-49,348,360 (hg38), as previously described[20], and contains ~15K gRNAs flanked by a 5'-NGG protospacer adjacent motifs (Table S1). Briefly, gRNA sequences with cloning adapters were synthesized by Agilent Technologies, amplified, and cloned into pCRISPRia-v2 (Addgene, 84832). The dCas9-ZIM3 plasmid was designed and cloned, as previously described[20]. The CRISPRn gRNA library contains 6000 gRNAs targeting 1349 transcription factors, chromatin modifiers, and immune genes of interest, with 593 non-targeting controls and 13 EGFP-targeting controls[24].

Lentivirus production

Lentiviruses containing the CRISPRi gRNA library, dCas9-ZIM3 construct, and CRISPRn gRNA library were generated as previously described[33]. Low passage number Human Embryonic Kidney 293T cells were thawed and cultured at 37°C and 5% CO_2 in DMEM, high glucose, GlutaMAX Supplement medium (Fisher Scientific, catalog no. 10566024) supplemented with 10% FBS, 100 U/mL Penicillin-Streptomycin (Fisher Scientific, catalog no. 15140122), 2 mM L-glutamine (Fisher Scientific, catalog no. 25030081), 10 mM HEPES (Sigma, catalog no. H0887-100ML), 1X MEM Non-Essential Amino Acids Solution (Fisher Scientific, catalog no. 11140050), and 1 mM Sodium Pyruvate (Fisher Scientific, catalog no. 11360070) for at least 3 passages, without exceeding 80% confluency. On day 0, 293T cells were seeded in a flat-bottom culture vessel at medium-high confluency in Opti-MEM I Reduced Serum Medium (Fisher Scientific, catalog no. 31985088) supplemented with 5% FBS, 100 U/mL Penicillin-Streptomycin (Fisher Scientific, catalog no. 15140122), 2 mM L-glutamine (Fisher Scientific, catalog no. 25030081), 1X MEM Non-Essential Amino Acids Solution (Fisher Scientific, catalog no. 11140050), and 1 mM Sodium Pyruvate (Fisher Scientific, catalog no. 11360070) to achieve 95% confluency following overnight incubation at 37°C and 5% CO_2 overnight. When cells reached approximately 95% confluency, transfection complexes were assembled. To assembled transfection complexes, supplement-free Opti-MEM (Fisher Scientific, catalog no. 31985088) was adjusted to room temperature. Lipofectamine3000 Mastermix was assembled by adding 0.79 μL Lipofectamine 3000 reagent (Fisher Scientific, catalog no. L3000075) per cm^2 of the 293T culture vessel to 1/8 293T culture volume of room temperature supplement-free Opti-MEM. In parallel, P3000 Mastermix was assembled by adding 125 ng psPAX2 (Addgene 12260) per cm^2 of the 293T culture vessel, 62.5 ng pMD2.G (Addgene 12259) per cm^2 of the 293T culture vessel, and 167 ng transfer plasmid (CRISPRi gRNA library, dCas9-ZIM3, or CRISPRn gRNA library) per cm^2 of the 293T culture vessel to 1/8 293T culture volume of room temperature supplement-free Opti-MEM. After addition of plasmids, 0.71 μL p3000 Reagent (Fisher Scientific, catalog no. L3000075) per cm^2 of the 293T culture vessel was added. Mastermixes

were mixed gently by inversion, and Lipofectamine3000 Mastermix was added dropwise to P3000 Mastermix, gently inverting to mix. The combined transfection mix was incubated at room temperature for 15 min. One-fourth volume of the 293T medium was removed, and the equivalent volume of transfection complex was added to 293T cultures and incubated for 6 hours at 37°C and 5% CO_2. After incubation, media was removed and replaced with fresh complete media with 1X ViralBoost Reagent (Alstem, catalog no. VB100) and incubated 18 hours at 37°C and 5% CO_2. Twenty-four hours after transfection, media was transferred to 50 mL centrifuge tubes and centrifuged at 300g for 5 min to remove cell debris. Supernatant was transferred to a new tube and stored at 4°C, and fresh complete media with 1X ViralBoost was gently replaced on 293T. Forty-eight hours post-transfection, media was collected again, as described, and combined with supernatant collected at 24-hours post-transfection. Lenti-X Concentrator (Takara Bio, catalog no. 631232) was added to combined supernatant, and lentiviral particles were concentrated according to manufacturer's protocol and resuspended in supplement-free Opti-MEM to 1% of the original culture volume. Lentiviral particles were aliquoted and frozen at -80°C, thawing immediately prior to use.

Intracellular flow cytometry staining

Approximately 5E4-3E5 cells per donor and cell type were transferred to a 96-well V-bottom plate, centrifuged at 300g for 5 minutes, and supernatant was removed. Cells were washed with 200 μL EasySep buffer and resuspended in 50 μL of staining solution containing Ghost Dye Red 780 Live/Dead stain (Tonbo, catalog no. 13-0865-T500) and antibodies targeting surface proteins of interest. Cells were incubated on ice for 20 minutes, protected from light. After staining, cells were washed by addition of 150 μL EasySep, centrifuged at 300g for 5 minutes, and supernatant was removed. Intracellular staining was conducted using the FOXP3 Fix/Perm Buffer Set (Biolegend, catalog no. 421403). Kit components were diluted in DPBS according to manufacturer's protocol. Cells were resuspended in 50 μL 1X FOXP3 Fix/Perm Buffer and incubated at room temperature for 30 minutes, protected from light. After fixation, cells were washed by addition of 150 μL 1X FOXP3 Perm Buffer, centrifuged at 300g for 5 minutes, and supernatant was removed. Cells were permeabilized in 200 μL 1X FOXP3 Perm Buffer for 15 minutes at room temperature, protected from light. Following permeabilization, cells were centrifuged at 300g for 5 minutes, and supernatant was removed. Cells were resuspended in 50 μL 1X FOXP3 Perm Buffer containing antibodies targeting intracellular proteins of interest and incubated 30 minutes at room temperature, protected from light. Following intracellular staining, cells were washed by addition of 150 μL 1X FOXP3 Perm Buffer, centrifuged at 300g for 5 minutes, and supernatant was removed. Cells were resuspended in 200 μL EasySep for flow cytometry. Stained cells were analyzed on an Attune NxT Flow Cytometer. For larger samples, volumes were adjusted to accommodate staining of higher cell numbers in 50 mL conical tubes.

CRISPRi screen

CRISPRi screens were conducted in Tconv and Treg from the same two donors, with a third donor used only in Tconv.

Lentiviral infection and selection. Twenty-four hours post-stimulation, cells were infected with titered dCas9-ZIM3 lentivirus, targeting approximately 80% infection, by addition to culture flasks. Cells and lentivirus were gently pipetted once with a large serological pipette to mix. Forty-eight hours post-stimulation, cells were infected with gRNA library lentivirus, targeting

approximately 60% infection, by addition to culture flasks and gently mixing. Twenty-four hours post-gRNA library lentivirus infection, viral media was removed, and cells were resuspended in media containing 1.5 ug/mL puromycin to select for cells with proper gRNA integration. Cells were cultured in puromycin-supplemented media for 48 hours.
Cell purity intracellular staining. Seven days post-stimulation, a small fraction of Treg and Tconv were removed from culture to assess cell population purity, and stained as described in *Intracellular flow cytometry staining*. Cells were stained using antibodies targeting CD4 (Biolegend, catalog no. 344634), FOXP3 (Biolegend, catalog no. 126406), and HELIOS (Biolegend, catalog no. 137216). Cells were gated on live cells and CD4+, and the percentage of FOXP3+HELIOS+ cells (Tregs) were compared to the percentage of FOXP3-HELIOS- cells (Tconvs).

Restimulation and cell sorting. Nine days post-stimulation, cells were restimulated at a 1:1 cell to bead ratio with CTS Dynabeads CD3/CD28 (Thermo Fisher Scientific, catalog no. 40203D). Forty-eight hours post-restimulation, beads were separated from cells using magnetic isolation. Tregs and Tconvs were counted, washed, and stained with Ghost Dye Red 780 Live/Dead stain (Tonbo, catalog no. 13-0865-T500) and antibodies targeting CD4 (Biolegend, catalog no. 344634), FOXP3 (Biolegend, catalog no. 126406) and HELIOS (Biolegend, catalog no. 137216), as described in *Intracellular flow cytometry staining*, with adjusted volumes to accommodate large cell numbers. Cells were sorted on lymphocytes, singlets, live cells, BFP+ (a marker of the gRNA library plasmid), and FOXP3 high and low bins that captured the top and bottom ~25% of FOXP3 expression in each cell type. Following sorting, cells were pelleted and lysed, and genomic DNA (gDNA) was extracted using phenol-chloroform gDNA extraction.

Library preparation and sequencing. Regions containing the lentivirally integrated gRNA were amplified using PCR with custom primers. PCR reactions were conducted using 2 μg gDNA per 50 μL reaction with 0.5 μM forward and reverse primers, 0.075 U/μL TaKaRa Ex Taq DNA polymerase (Takara Bio, catalog no. RR001C), 0.2 mM dNTP, and 1X Ex Taq Buffer and amplified under the following cycling conditions: 1 min at 95°C, (30 s at 95°C, 30 s at 60°C, 30 s at 72°C) x 25 cycles, 10 min at 72°C, hold at 4°C. Following amplification, aliquots of individual samples were pooled, and primer dimers removed using a 1.4X SPRI bead cleanup. Proper amplification and concentration were assessed using Qubit quantification and DS1000 High Sensitivity Tapestation analysis, according to manufacturers' protocols. Samples were pooled equimolarly and sequenced on an Illumina HiSeq4000 instrument using a custom sequencing primer.

CRISPRi screen analysis
To acquire genomic coordinates of the CRISPRi library gRNAs, gRNA sequences were mapped to the expanded *FOXP3* locus (chrX:49200000-49348394, human genome hg38) using bwa (v0.7.18)[34] with the following command and specifications: bwa aln -n 0. Aligned SAM files were converted to BAM files and indexed using samtools (v1.10) and converted to a BED file containing genomic coordinates using bedtools (v2.31.1) bamtobed. 14,889 gRNAs were successfully mapped, and the midpoint of each gRNA was selected as the coordinate for plotting.

CRISPRi pooled screens were analyzed using MAGeCK[35] (v0.5.9.5). A count file containing individual gRNA abundance across all donors was generated using the command mageck count

with specification –norm-method none (Table S2). Differential enrichment of gRNAs was determined using DESeq2 (v1.40.2), as described previously[20] (Table S3, Table S4). Guide RNAs with fewer than ten reads were excluded. Guide RNAs not mapping to the *FOXP3* locus were excluded from visualization.

To decrease noise and enable comparison of individual donor replicates, count files were generated for individual donor samples, as described in combined analyses. Guide RNAs not mapping to the *FOXP3* locus were excluded. Neighboring gRNAs were grouped into sliding 500 bp bins, shifted 50 bp at a time, as "genes", and gRNAs with less than 10 reads across 5+ samples were excluded from analysis. Guide RNA "gene" bins from individual donors with significant differential enrichment between low and high FOXP3 FACS bins were identified using the binned count file with the command mageck test. Donor 2 in the Tconv screen showed no low bin enrichment at the *FOXP3* TSS (Figure S1D) and was subsequently excluded from the combined donor analysis described above.

Cas9 RNP assembly

To assemble RNPs for individual edits and paired deletions, individual custom crRNAs targeting regions of interest (Dharmacon) and Edit-R CRISPR-Cas9 Synthetic tracrRNA (Dharmacon, catalog no. U-002005-20) were resuspended in Nuclease-Free Duplex Buffer (IDT, catalog no. 11-01-03-01) at 160 uM, complexed at a 1:1 molar ratio to create a 80 μM solution of RNA complexes, and incubated 30 min at 37°C. Single-stranded oligonucleotides (ssODN; 100 μM stock, sequence: TTAGCTCTGTTTACGTCCCAGCGGGCATGAGAGTAACAAGAGGGTGTGGTAATATTA CGGTACCGAGCACTATCGATACAATATGTGTCATACGGACACG) were mixed at a 1:1 molar ratio with complexed RNA and incubated 5 min at 37°C. Cas9 protein (Berkeley Macrolab, 40 μM stock) was slowly added at a 1:1 molar ratio of Cas9 to RNA complexes, mixed thoroughly, and incubated 15 min at 37°C. For RNPs used in paired deletions, individually assembled RNPs were mixed 1:1 with the appropriate RNP pair. RNPs were frozen at -80°C and thawed at room temperature prior to use.

RNP electroporation

Cells (Tregs and/or Tconvs) were isolated and stimulated as described above. Forty-eight hours post-stimulation, cells were counted, pelleted via centrifugation, and resuspended at 2E4-7.5E4 cells/μL in freshly supplemented P3 Primary Cell Nucleofector Solution (Lonza, catalog no. V4SP-3096). For single RNP edits, 20 μL cells were mixed with 3.5 μL RNP, and 22 μL was transferred to a 96-well Nucleocuvette Plate (Lonza, catalog no. V4SP-3096). For paired RNP deletions, 20 μL cells were mixed with 7 μL paired RNPs, and 24.5 μL was transferred to a 96-well Nucleocuvette Plate (Lonza, catalog no. V4SP-3096). Cells were nucleofected using a Lonza 4D 96-well electroporation system with pulse code EO-115 (Treg) or EH-115 (Tconv). Immediately after electroporation, 80 μL pre-warmed media was added to each well, and the cells were incubated for 15 min at 37°C. Following incubation, cells were plated at approximately 1E6 cells/mL for culture.

CRISPRi screen validation

Cas9 RNP assembly and electroporation. To validate CRISPRi screening in an arrayed format, paired crRNAs tiling CRISPRi-responsive and control regions were designed to delete

approximately 1 kb of DNA. Single (3) and paired (2) crRNAs targeting the AAVS1 safe-harbor locus were designed as negative controls, and single crRNAs from the Brunello Library targeting *FOXP3* exons (4) were included as positive controls[36]. Additional single crRNAs from the Brunello Library targeting *PPP1R3F* exons (4) were included to control for effects of gene KO when tiling across the TSS region[36]. RNPs were assembled as described in *Cas9 RNP assembly*. Forty-eight hours post-stimulation, Tregs and Tconv were electroporated as described in *RNP electroporation*.

Flow cytometry analysis of arrayed validation. Nine days post-stimulation, a portion of cells were stained with Ghost Dye Red 780 Live/Dead stain (Tonbo, catalog no. 13-0865-T500) and antibodies targeting CD4 (Biolegend, catalog no. 344620), CD25 (Tonbo, catalog no. 20-0259-T100), FOXP3 (Biolegend, catalog no. 126406), and HELIOS (Biolegend, catalog no. 137216), as described in *Intracellular flow cytometry staining*, above. Remaining unstained cells were restimulated with CTS Dynabeads CD3/CD28 beads (Thermo Fisher Scientific, catalog no. 40203D) at a cell to bead ratio of 1:1. Forty-eight hours post-restimulation, beads were removed via magnetic separation, and cells were stained as described on day 9. Flow cytometry data from stained cells was collected on an Attune NxT Flow Cytometer. Analysis with gating on lymphocytes, singlets, live cells, and CD4+ cells was conducted using FlowJo. Flow cytometry statistics were exported via the FlowJo Table Editor and visualized in R using ggplot2 (v3.5.1). For arrayed validation dot plots, FOXP3 MFI (Tregs) or %FOXP3+ cells (Tconvs) in KOs from each donor were normalized to the mean of the donor-matched AAVS1 controls.

Stimulation ATAC-seq analysis

Fastqs from previously published ATAC-seq datasets[22] corresponding to unstimulated and stimulated CD4 Effector T cells (Tconv) and Regulatory T cells (Treg) were downloaded from GEO series GSE118189. Fastq files were processed as previously described[37]. Briefly, adapters were trimmed using fastp, and reads were aligned to the hg38 reference genome using hisat2. Reads were deduplicated using picard. Peaks were called from each sample using MACS2. ATAC fragments for each sample were converted into bigwig files normalized by the number of reads in transcription start sites in each sample using `rtracklayer::export` in R. Normalized bigwigs from a representative donor (GSM3320328, 1003-Effector_CD4pos_T-U; GSM3320329, 1003-Effector_CD4pos_T-S; GSM3320338, 1003-Regulatory_T-U; GSM3320339, 1003-Regulatory_T-S) were visualized in R using ggplot2 (v3.5.1).

CRISPRn screen

CRISPRn screens were conducted in Tconv isolated from three healthy donors. Screens were conducted as previously described[24], with minor modifications.

Lentiviral infection and electroporation. Cells were isolated and stimulated, as described above. Twenty-four hours post-stimulation, cells were infected with titered gRNA library lentivirus, targeting approximately 85% infection, by addition to culture flasks. Cells and lentivirus were gently pipetted once with a large serological pipette to mix. Twenty-four hours post-gRNA library lentivirus infection, viral media was removed, and cells were washed with 1X volume pre-warmed media and plated at approximately 1E6 cells/mL.

Cas9 RNPs were assembled as described in *Cas9 RNP assembly*, above, using a Guide Swap crRNA method[38] (Edit-R crRNA nontargeting Control 3, Dharmacon, catalog no. U-007503-01-

05). Seventy-two hours post-stimulation, cells were pelleted, and resuspended at 7.5E4 cells/μL in freshly supplemented P3 Primary Cell Nucleofector Solution (Lonza, catalog no. V4SP-3096). 20 μL of cell were mixed with 7 μL RNP, and 25 μL was transferred to a 96-well Nucleocuvette Plate (Lonza, catalog no. V4SP-3096) and electroporated, as described in *RNP electroporation*, above.

Restimulation and cell sorting. Nine days post-stimulation, cells were restimulated at a 1:1 cell to bead ratio with CTS Dynabeads CD3/CD28 (Thermo Fisher Scientific, catalog no. 40203D). Forty-eight hours post-restimulation, beads were separated from cells using magnetic isolation. Cells were counted and stained with Ghost Dye Red 780 Live/Dead stain (Tonbo, catalog no. 13-0865-T500) and antibodies targeting FOXP3 (Biolegend, catalog no. 320116) and HELIOS (Biolegend, catalog no. 137216), as described in *Intracellular flow cytometry staining*, with adjusted volumes to accommodate large cell numbers. Cells were sorted on lymphocytes, singlets (x2), live cells, GFP+ (a marker of the gRNA library plasmid), and FOXP3 high and low bins that captured the top and bottom 25% of FOXP3 expression. Following sorting, cells were pelleted and lysed, and gDNA was extracted using phenol-chloroform gDNA extraction.
Library preparation and sequencing. Regions containing the lentivirally integrated gRNA were amplified using PCR with custom primers. PCR reactions were conducted using 1.75 μg gDNA per 50 μL reaction with 0.25 μM forward and reverse primers and 1X NEBNext Ultra II Q5 Master Mix (New England Biolabs, catalog no. M0544). Reactions were amplified under the following cycling conditions: 3 min at 98°C, (10 s at 98°C, 10 s at 63°C, 25 s at 72°C) x 23 cycles, 2 min at 72°C, hold at 4°C. Following amplification, aliquots of individual samples were pooled, and primer dimers removed using a 1.25X SPRI bead cleanup. Proper amplification and concentration were assessed using Qubit quantification and DS1000 High Sensitivity Tapestation analysis, according to manufacturers' protocols. Samples were pooled equimolarly and sequenced on an Illumina HiSeq4000 instrument using a custom sequencing primer.

CRISPRn screen analysis
CRISPRn pooled screens were analyzed using MAGeCK[35] (v0.5.9.5). A count file containing individual gRNA abundance across all donors was generated using the command mageck count with specification –norm-method none (Table S5). Differentially enriched gRNAs and significantly enriched genes in high and low bins were identified using the command mageck test, specifying –sort-criteria pos (Table S6, Table S7).

CRISPRn screen validation
Top FOXP3 maintenance and suppressive regulators were selected for arrayed validation, and two crRNAs were selected for each regulator. Six crRNAs targeting the AAVS1 locus were additionally included as negative controls. Cas9 RNPs were assembled as described in *Cas9 RNP assembly*, above. Human Tconv from two healthy donors were isolated and stimulated as described above. Forty-eight hours post-stimulation, cells were electroporated with trans-regulator targeting RNPs, as described in *RNP electroporation*, above. Nine days post-stimulation, a portion of cells were stained with Ghost Dye Red 780 Live/Dead stain (Tonbo, catalog no. 13-0865-T500) and antibodies targeting CD4 (Biolegend, catalog no. 344634), FOXP3 (Biolegend, catalog no. 126406), and HELIOS (Biolegend, catalog no. 137216), as described in *Intracellular flow cytometry staining*, above. Remaining unstained cells was restimulated with 12.5 uL/mL Immunocult Human CD3/CD28/CD2 T Cell Activator

(STEMCELL Technologies, catalog no. 10970). Forty-eight hours post-restimulation, cells were stained as described on day 9. Flow cytometry data from stained cells was collected on an Attune NxT Flow Cytometer. Analysis with gating on lymphocytes, singlets, live cells, and CD4+ cells was conducted using FlowJo. Flow cytometry statistics were exported via the FlowJo Table Editor and visualized in R using ggplot2 (v3.5.1). For arrayed validation bar plots, raw %FOXP3+ cells or FOXP3 MFI normalized to the mean of the donor-matched AAVS1 controls were shown.

Genotyping of arrayed CRISPRn knock-outs

Genomic DNA from 3E4-2E5 cells was isolated from arrayed samples using QuickExtract DNA Extraction Solution (Biosearch Technologies, catalog no. QE09050), using manufacturer's protocol with reduced reagent volume to accommodate processing in a 96-well PCR plate. Paired PCR primers were designed flanking the gRNA cut site to generate an amplicon of approximately 200 bp. PCR reactions were conducted for each sample using 4 μL QuickExtract-isolated gDNA per 25 μL reaction, 0.5 μM forward and reverse primers, and 1X NEBNext Ultra II Q5 Master Mix (New England Biolabs, catalog no. M0544). Reactions were amplified under the following cycling conditions: 3 min at 98°C, (20 s at 94°C, 20 s at 65-57.5°C (with 0.5°C incremental decreases per cycle), 1 min at 72°C) x 15 cycles, (20 s at 94°C, 20 s at 58°C, 1 min at 72°C) x 20 cycles, 10 min at 72°C, hold at 4°C. Amplified DNA was diluted 1:200, and 1 μL was used per 25 μL of a second PCR amplification with 1 μM forward and reverse primers and 1X NEBNext Ultra II Q5 Master Mix to attached sequencing adapters and indices. Reactions were amplified under the following cycling conditions: 30 s at 98°C, (10 s at 98°C, 30 s at 60°C, 30 s at 72°C) x 12 cycles, 2 min at 72°C, hold at 4°C. Following amplification, samples were pooled in equal volume, and primer dimers were removed using a 1.3X SPRI bead cleanup. Proper amplification and concentration were assessed using Qubit quantification and DS1000 High Sensitivity Tapestation analysis, according to manufacturers' protocols. The pooled samples were sequenced on an Illumina MiSeq instrument with PE 150 reads. Analysis of editing efficiency was performed using CRISPResso2[39] (v2.2.12), using the command CRISPRessoBatch –batch_settings [crispresso_samplesheet] –skip_failed –n_processes 4 –exclude_bp_from_left 0 –exclude_bp_from_right 0 –plot_window_size 10.

Transcription factor binding site analysis

Motif analysis was conducted as described[24], with minor modifications. Briefly, datasets containing human or human-predicted position weight matrices for human transcription factors were acquired from JASPAR2020[27] (v0.99.10) using TFBSTools (v1.38.0) in R or sourced from CisBP (*Homo sapiens*, downloaded 09-29-2020)[26]. Motif sites in a region of interest were identified using 'matchMotifs' from motifatchr (v1.22.0) using default settings and specifying the genome as Bsgenome.Hsapien.UCSC.hg38 (v1.4.5).

KO ATAC-seq analysis

KO ATAC-seq data was analyzed as previously described[24], but using only ATAC-seq data from male donors and without removal of reads mapping to ChrX. Briefly, sequencing read adapters were trimmed using cutadapt (v2.10) to a minimum length of 20 bp, and reads were mapped to GRCh38 using bowtie2 (v2.4.1). Low-quality reads were filtered using SAMtools (v1.10), reads mapping to ENCODE blacklist regions removed with bedtools (v2.29.2), duplicates removed using picard (v2.23.3), and reads mapping to chrM and chrY were removed. Called peaks were

generated using MACS2 (v2.2.7.1), and a consensus peak file was generated. The GenomicAlignments (v1.36.0) summarizeOverlaps function was used to count Tn5 insertion sites overlapping each consensus peak to generate a count matrix. Significantly differentially accessible peaks over AAVS1 control samples were identified using DESeq2 (v1.40.2). Scaling factors for ATAC-seq bigwig visualization were generated using the DESeq2 (v1.40.2) estimateSizeFactorsForMatrix function, as previously described[20]. Donor replicate files for each KO were merged into consensus bigwig files and visualized in R using ggplot2 (v3.5.1).

KO RNA-seq analysis

A pre-processed KO RNA-seq differential expression analysis file was downloaded from ref[24]. Processing of this file was described in (ref[24]): fastq adapters were trimmed using cutadapt (v2.10), reads were mapped to human genome GRCh38 using STAR (v2.7.5b), excluding multi-mapping reads, UMIs extracted using umi_tools (v1.0.1), reads deduplicated using umi_tools, and Gencode v35 gene counts generated using featureCounts (v2.0.1). Differentially expressed genes for KO over AAVS1 controls were identified using Limma (v3.44.3).

ChIP-seq analysis

Pre-processed ChIP-seq bigwigs were downloaded from ChIP-Atlas[40]. ChIP-Atlas processing uses Bowtie2 for alignment to the human genome GRCh38, SAMtools to convert to BAM format, sort, and remove PCR duplicates, bedtools to calculate coverage scores in reads per million mapped reads, MACS2 to call peaks, and the UCSC BedGraphToBigWig tool to generate bigwig coverage files. ChIP-seq data for the indicated cell type were generated in the following papers and are available at the listed GEO sample accession code: BCL11B (primary T-ALL with enhanced BCL11B expression, GSM5024541, ref.[41]), ETS1 (Jurkat clone E6-1, GSM449525, ref.[42]), GABPA (Jurkats, GSM1193662, ref.[43]), MBD2 (K-562, GSM2527611, ref.[44]), GATA3 (in vitro differentiated primary human Th1 cells, GSM776558, ref.[32]), STAT5B (human CD4+ T cells stimulated with IL-2 for 1 hour, GSM671402, ref.[45]), TFDP1 (MM.1S, GSM2132551, ref.[46]), YY1 (T-ALL cell line DND-41 treated with DMSO, GSM5282087, ref.[47]), and ZNF143 (CUTLL1, GSM732907, ref.[48]). Bigwig files were visualized in R using ggplot2 (v3.5.1) and auto scaled to the locus shown.

Plots and Genomic Tracks

Gene tracks were plotted from a subset of GENCODE hg38 knownGene annotations downloaded from the UCSC Genome Browser (ref.[49]) Table Browser and visualized in R using ggplot2 (v3.5.1). PhyloP 100way conservation track data were sourced from phyloP100way downloaded from the UCSC Genome Browser Table Browser and visualized in R with ggplot2 using 25 bp window bins. Select schematics incorporated images from https://www.biorender.com.

Data accessibility

Sequencing data is available upon request and will be deposited to NCBI Gene Expression Omnibus prior to publication.

Code accessibility

Custom code is available upon request and will be deposited to a public repository prior to publication.

References

1. Wang, J., Ioan-Facsinay, A., van der Voort, E. I. H., Huizinga, T. W. J. & Toes, R. E. M. Transient expression of FOXP3 in human activated nonregulatory CD4+ T cells. *Eur. J. Immunol.* **37**, 129–138 (2007).
2. Allan, S. E. *et al*. Activation-induced FOXP3 in human T effector cells does not suppress proliferation or cytokine production. *Int. Immunol.* **19**, 345–354 (2007).
3. Gavin, M. A. *et al*. Single-cell analysis of normal and FOXP3-mutant human T cells: FOXP3 expression without regulatory T cell development. *Proc. Natl. Acad. Sci. U. S. A.* **103**, 6659–6664 (2006).
4. Fontenot, J. D., Gavin, M. A. & Rudensky, A. Y. Foxp3 programs the development and function of CD4+CD25+ regulatory T cells. *Nat. Immunol.* **4**, 330–336 (2003).
5. Hori, S., Nomura, T. & Sakaguchi, S. Control of regulatory T cell development by the transcription factor Foxp3. *Science (80-.).* **299**, 1057–1061 (2003).
6. Voss, K. *et al*. FOXP3 protects conventional human T cells from premature restimulation-induced cell death. *Cell. Mol. Immunol.* **18**, 194–205 (2021).
7. Dikiy, S. *et al*. A distal Foxp3 enhancer enables interleukin-2 dependent thymic Treg cell lineage commitment for robust immune tolerance. *Immunity* **54**, 931–946 (2021).
8. Kawakami, R. *et al*. Distinct Foxp3 enhancer elements coordinate development, maintenance, and function of regulatory T cells. *Immunity* **54**, 947–961 (2021).
9. Zheng, Y. *et al*. Role of conserved non-coding DNA elements in the Foxp3 gene in regulatory T-cell fate. *Nature* **463**, 808–812 (2010).
10. Kim, H.-P. & Leonard, W. J. CREB/ATF-dependent T cell receptor-induced FoxP3 gene expression: A role for DNA methylation. *J. Exp. Med.* **204**, 1543–1551 (2007).
11. Tone, Y. *et al*. Smad3 and NFAT cooperate to induce Foxp3 expression through its enhancer. *Nat. Immunol.* **9**, 194–202 (2008).
12. Vaeth, M. *et al*. Dependence on nuclear factor of activated T-cells (NFAT) levels discriminates conventional T cells from Foxp3+ regulatory T cells. *Proc. Natl. Acad. Sci. U. S. A.* **109**, 16258–16263 (2012).
13. Wang, Y., Su, M. A. & Wan, Y. Y. An Essential Role of the Transcription Factor GATA-3 for the Function of Regulatory T Cells. *Immunity* **35**, 337–348 (2011).
14. Cortez, J. T. *et al*. CRISPR screen in regulatory T cells reveals modulators of Foxp3. *Nature* **582**, 416–420 (2020).
15. Loo, C.-S. *et al*. A Genome-wide CRISPR Screen Reveals a Role for the Non-canonical Nucleosome-Remodeling BAF Complex in Foxp3 Expression and Regulatory T Cell Function. *Immunity* **53**, 143–157 (2020).
16. Schumann, K. *et al*. Functional CRISPR dissection of gene networks controlling human regulatory T cell identity. *Nat. Immunol.* **21**, 1456–1466 (2020).
17. Baron, U. *et al*. DNA demethylation in the human FOXP3 locus discriminates regulatory T cells from activated FOXP3+ conventional T cells. *Eur. J. Immunol.* **37**, 2378–2389 (2007).
18. Janson, P. C. J. *et al*. FOXP3 promoter demethylation reveals the committed Treg population in humans. *PLoS One* **3**, e1612 (2008).
19. Nagar, M. *et al*. Epigenetic inheritance of DNA methylation limits activation-induced expression of FOXP3 in conventional human CD25-CD4+ T cells. *Int. Immunol.* **20**, 1041–1055 (2008).

20. Mowery, C. T. *et al*. Systematic decoding of cis gene regulation defines context-dependent control of the multi-gene costimulatory receptor locus in human T cells. *Nat. Genet.* **56**, 1156–1167 (2024).
21. Zemmour, D., Pratama, A., Loughhead, S. M., Mathis, Di. & Benoist, C. Flicr, a long noncoding RNA, modulates Foxp3 expression and autoimmunity. *Proc. Natl. Acad. Sci. U. S. A.* **114**, E3472–E3480 (2017).
22. Calderon, D. *et al*. Landscape of stimulation-responsive chromatin across diverse human immune cells. *Nat. Genet.* **51**, 1494–1505 (2019).
23. Shifrut, E. *et al*. Genome-wide CRISPR Screens in Primary Human T Cells Reveal Key Regulators of Immune Function. *Cell* **175**, 1958–1971 (2018).
24. Freimer, J. W. *et al*. Systematic discovery and perturbation of regulatory genes in human T cells reveals the architecture of immune networks. *Nat. Genet.* **54**, 1133–1144 (2022).
25. Zorn, E. *et al*. IL-2 regulates FOXP3 expression in human CD4+CD25+ regulatory T cells through a STAT-dependent mechanism and induces the expansion of these cells in vivo. *Blood* **108**, 1571–1579 (2006).
26. Weirauch, M. T. *et al*. Determination and inference of eukaryotic transcription factor sequence specificity. *Cell* **158**, 1431–1443 (2014).
27. Baranasic, D. JASPAR2020: Data package for JASPAR database (version 2020). R package version 0.99.8. (2020).
28. Verheul, T. C. J., van Hijfte, L., Perenthaler, E. & Barakat, T. S. The Why of YY1: Mechanisms of Transcriptional Regulation by Yin Yang 1. *Front. Cell Dev. Biol.* **8**, 592164 (2020).
29. Weintraub, A. S. *et al*. YY1 Is a Structural Regulator of Enhancer-Promoter Loops. *Cell* **172**, 1573–1588 (2017).
30. Shin, H. M. *et al*. Transient expression of ZBTB32 in anti-viral CD8+ T cells limits the magnitude of the effector response and the generation of memory. *PLoS Pathog.* **13**, e1006544 (2017).
31. Omori, M. *et al*. CD8 T cell-specific downregulation of histone hyperacetylation and gene activation of the IL-4 gene locus by ROG, repressor of GATA. *Immunity* **19**, 281–294 (2003).
32. Kanhere, A. *et al*. T-bet and GATA3 orchestrate Th1 and Th2 differentiation through lineage-specific targeting of distal regulatory elements. *Nat. Commun.* **3**, 1268 (2012).
33. Schmidt, R. *et al*. CRISPR activation and interference screens decode stimulation responses in primary human T cells. *Science (80-.).* **375**, eabj4008 (2022).
34. Li, H. & Durbin, R. Fast and accurate short read alignment with Burrows-Wheeler transform. *Bioinformatics* **25**, 1754–1760 (2009).
35. Li, W. *et al*. MAGeCK enables robust identification of essential genes from genome-scale CRISPR/Cas9 knockout screens. *Genome Biol.* **15**, 554 (2014).
36. Sanson, K. R. *et al*. Optimized libraries for CRISPR-Cas9 genetic screens with multiple modalities. *Nat. Commun.* **9**, 5416 (2018).
37. Belk, J. A. *et al*. Genome-wide CRISPR screens of T cell exhaustion identify chromatin remodeling factors that limit T cell persistence. *Cancer Cell* **40**, 768–786 (2022).
38. Ting, P. Y. *et al*. Guide Swap enables genome-scale pooled CRISPR–Cas9 screening in human primary cells. *Nat. Methods* **15**, 941–946 (2018).
39. Clement, K. *et al*. CRISPResso2 provides accurate and rapid genome editing sequence analysis. *Nat. Biotechnol.* **37**, 215–226 (2019).

40. Oki, S. *et al*. ChIP-Atlas: a data-mining suite powered by full integration of public ChIP-seq data. *EMBO Rep*. **19**, e46255 (2018).
41. Montefiori, L. E. *et al*. Enhancer hijacking drives oncogenic BCL11B expression in lineage-ambiguous stem cell leukemia. *Cancer Discov*. **11**, 2846–2867 (2021).
42. Hollenhorst, P. C. *et al*. DNA specificity determinants associate with distinct transcription factor functions. *PLoS Genet*. **5**, e1000778 (2009).
43. Sharma, N. L. *et al*. The ETS family member GABPα modulates androgen receptor signalling and mediates an aggressive phenotype in prostate cancer. *Nucleic Acids Res*. **42**, 6256–6269 (2014).
44. ENCODE Project Consortium. An integrated encyclopedia of DNA elements in the human genome. *Nature* **489**, 57–74 (2012).
45. Liao, W., Lin, J.-X., Wang, L., Li, P. & Leonard, W. J. Modulation of cytokine receptors by IL-2 broadly regulates differentiation into helper T cell lineages. *Nat. Immunol*. **12**, 551–559 (2011).
46. Fulciniti, M. *et al*. Non-overlapping Control of Transcriptome by Promoter- and Super-Enhancer-Associated Dependencies in Multiple Myeloma. *Cell Rep*. **25**, 3693–3705 (2018).
47. Zhou, Y. *et al*. EBF1 nuclear repositioning instructs chromatin refolding to promote therapy resistance in T leukemic cells. *Mol. Cell* **82**, 1003–1020 (2022).
48. Wang, H. *et al*. Genome-wide analysis reveals conserved and divergent features of Notch1/RBPJ binding in human and murine T-lymphoblastic leukemia cells. *Proc. Natl. Acad. Sci. U. S. A*. **108**, 14908–14913 (2011).
49. Nassar, L. R. *et al*. The UCSC Genome Browser database: 2023 update. *Nucleic Acids Res*. **51**, D1188–D1195 (2023).

Acknowledgements
We thank all members of the Marson Lab for valuable input and discussion. We thank Jane Srivastava of the Gladstone Flow Cytometry Core for technical help and support with FACS, which is supported by NIH S10 RR028962 and the James B. Pendleton Charitable Trust. We also acknowledge the Juvenile Diabetes Research Foundation and the Larry L. Hillblom Foundation for their support of this work. A.M. received funding from the Simons Foundation, Lloyd J. Old STAR Award (Cancer Research Institute), Parker Institute for Cancer Immunotherapy, Innovative Genomics Institute, Larry L. Hillblom Foundation (grant no. 2020-D-002-NET), and Northern California JDRF Center of Excellence. A.M. received gifts from the Byers family, Karen Jordan, and the CRISPR Cures for Cancer Initiative. J.A.B. was supported by the Hanna Gray Fellow program of the Howard Hughes Medical Institute. C.T.M. is a UCSF ImmunoX Computational Immunology Fellow, is supported by NIH grant F30AI157167, and has received support from NIH grants T32DK007418 and T32GM007618. B.G.G. was supported by the IGI-AstraZeneca Postdoctoral Fellowship. J.E.C. is supported by the NOMIS Foundation, the Lotte and Adolf Hotz-Sprenger Stiftung, the Swiss National Science Foundation (project grants 310030_188858 and 310030_201160), and the European Research Council (ERC) under the European Union's Horizon 2020 research and innovation program (grant agreement No 855741, DDREAMM).

Author Contributions

J.M.U. and A.M. conceptualized the study. J.M.U, M.M.A., and R.D. conducted experiments. J.M.U. and V.N. sorted cells in screening experiments. D.R.S, B.G.G., G.L.C., and J.E.C designed and generated the CRISPRi library. J.A.B. performed stimulation ATAC-seq analysis. H.Y.C. supervised stimulation ATAC-seq analysis. J.M.U. performed data analysis and visualization. M.M.A. and C.T.M provided analysis direction. M.M.A. helped design experiments. J.M.U wrote the original manuscript. J.M.U and A.M. edited the manuscript. A.M. provided resources, acquired funding, and supervised the study.

Competing Interests Declaration

A.M. is a cofounder of Site Tx, Arsenal Biosciences, Spotlight Therapeutics and Survey Genomics, serves on the boards of directors at Site Tx, Spotlight Therapeutics and Survey Genomics, is a member of the scientific advisory boards of Site Tx, Arsenal Biosciences, Cellanome, Spotlight Therapeutics, Survey Genomics, NewLimit, Amgen, and Tenaya, owns stock in Arsenal Biosciences, Site Tx, Cellanome, Spotlight Therapeutics, NewLimit, Survey Genomics, Tenaya and Lightcast and has received fees from Site Tx, Arsenal Biosciences, Cellanome, Spotlight Therapeutics, NewLimit, Gilead, Pfizer, 23andMe, PACT Pharma, Juno Therapeutics, Tenaya, Lightcast, Trizell, Vertex, Merck, Amgen, Genentech, GLG, ClearView Healthcare, AlphaSights, Rupert Case Management, Bernstein and ALDA. A.M. is an investor in and informal advisor to Offline Ventures and a client of EPIQ. The Marson laboratory has received research support from the Parker Institute for Cancer Immunotherapy, the Emerson Collective, Arc Institute, Juno Therapeutics, Epinomics, Sanofi, GlaxoSmithKline, Gilead and Anthem and reagents from Genscript and Illumina. C.T.M. is a Bio+Health Venture Fellow at Andreessen Horowitz. J.E.C. is a co-founder and SAB member of Serac Biosciences and an SAB member of Mission Therapeutics, Relation Therapeutics, Hornet Bio, and Kano Therapeutics. The lab of J.E.C. has funded collaborations with Allogene, Cimeio, and Serac. H.Y.C. is a co-founder of Accent Therapeutics, Boundless Bio, Cartography Biosciences, and Orbital Therapeutics, and is an advisor of 10x Genomics, Arsenal Bio, Chroma Medicine, Exai Bio, and Spring Discovery.

Materials and Correspondence

Correspondence and requests for material should be addressed to Alexander Marson (alex.marson@gladstone.ucsf.edu).

Figure Legends

Figure 1. CRISPRi tiling screen identifies shared and cell type-specific cis-regulators of FOXP3.

a. Schematic depicting CRISPRi-based screens for FOXP3 cis-regulators. **b.** CRISPRi *FOXP3* locus-tiling screen -log10(p-value) of gRNA enrichment in FOXP3 high vs. low FACS bins in Treg (top) and Tconv (bottom). *Blue*, gRNA enriched in FOXP3 High FACS bin. *Red*, gRNA enriched in FOXP3 Low FACS bin. *Outlined*, adjusted p-value is less than or equal to 0.05. Treg conserved noncoding sequences CNS0 and CNS2, *FOXP3* TSS, and novel Tconv enhancer, TcNS+, are highlighted in grey. Treg, $n = 2$ donors; Tconv, $n = 2$ donors. Conservation track depicts vertebrate PhyloP 100-way conservation. **c**-**d.** Arrayed validation of *FOXP3* TSS, FLICR, CNS0, and TcNS+ region-associated CRISPRi-responsive elements with paired Cas9 RNPs plotted along the *FOXP3* locus at 0 hours (Rest) and 48 hours (Stim) post-stimulation in Tregs (**c**) and Tconv (**d**). Locations of tiled deletions are indicated as tiles 1-24 and indicated by

line segments in (c) and (d). Lines indicate log2 fold change in mean FOXP3 MFI in Tregs (c) or %FOXP3+ Tconvs (d) in deletions vs. donor-specific paired AAVS1 gRNA controls. Points indicate individual replicates of tiled deletions (Treg n = 2 donors; Tconv n= 3 donors). Positive cis-elements CNS0, the *FOXP3* TSS, and TcNS+ are highlighted in red. Negative cis-element TcNS- is highlighted in blue. Heatmaps depict screen mean log2 fold change in gRNA enrichment in FOXP3 high vs. low bins, summarized over 100 bp windows across the locus. **e.** Representative flow plots depicting FOXP3 expression with Tile 14 and paired AAVS1 deletions in resting Tconv. Numbers indicate %FOXP3+ cells. Tile number corresponds to Tiled Deletions in (c, d). **f.** Normalized percentage FOXP3+ Tconv (top) or FOXP3 MFI in Tregs (bottom) in PPP1R3F or FOXP3 KO vs. AAVS1 KO controls. Stars indicate significant normalized change in %FOXP3+/FOXP3 MFI relative to AAVS1-targeting controls using a one-way ANOVA followed by Dunnett's test (*: $P \leq 0.05$; **: $P \leq 0.01$; ***: $P \leq 0.001$; Tconv, n = 3 donors; Treg, n = 2 donors, x 4 gRNAs per target or 3 AAVS1-targeting gRNA controls).

Figure 2. CRISPRn transcription factor screens identify trans-regulators of FOXP3 in Tconv.

a. Schematic depicting CRISPRn-based screens for FOXP3 trans-regulators in Tconvs. **b.** Volcano plot of log2 fold change of gene gRNA enrichment in FOXP3 high vs. low FACS bins versus -log10 of p-value. Color of points indicates significance (FDR ≤ 0.05). *Blue*, significantly enriched in FOXP3 high FACS bin. *Red*, significantly enriched in FOXP3 low FACS bin. *Gray*, not significant (n = 3 donors). **c.** *Top*, log2 fold change of individual gRNA enrichment in FOXP3 high vs. low FACS bins for significant FOXP3 maintenance and suppressive regulators (FDR ≤ 0.05; n = 3 donors). gRNAs corresponding to the labelled significant gene are colored blue (gene enriched in FOXP3 high bin), red (gene enriched in FOXP3 low bin), or gray (non-targeting control gRNA). *Bottom*, distribution of gRNA in screen. **d.** Arrayed validation of %FOXP3+ cells with KO of top FOXP3 maintenance and suppressive regulators at 0 hours (resting) and 48 hours (stimulated) post-stimulation in Tconvs. Color indicates directional effect in screen (n = 2 donors x 2 gRNAs per target or 6 gRNAs targeting AAVS1). **e.** Representative flow plots of AAVS1, GATA3, ETS1, and MBD2 KO in Tconvs at 48 hours post-stimulation. Numbers indicate %FOXP3+ cells.

Figure 3. KO of positive and negative trans-regulators change accessibility at CNS0 and TcNS+.

a. Predicted transcription factor binding sites of positive FOXP3 trans-regulators (top, red) and negative FOXP3 trans-regulators (bottom, blue) plotted along the *FOXP3* locus. Positive cis-elements CNS0, the *FOXP3* TSS, and TcNS+ are highlighted in red. Negative cis-element TcNS- is highlighted in blue. **b.** Publicly available ChIP-seq datasets in indicated T cells or T cell-based cell lines targeting positive (red) and negative (blue) trans-regulators of FOXP3. Cis-elements are labelled, as described in (a). **c.** Publicly available ChIP-seq datasets in indicated hematopoietic cell lines targeting negative (blue) trans-regulators of FOXP3. Cis-elements are labelled, as described in (a). **d.** Effect of trans-regulator KO on DNA accessibility[24] at the *FOXP3* locus. *Red*, accessibility with indicated positive regulator KO. *Blue*, accessibility with indicated negative regulator KO. *Gray*, accessibility in AAVS1 controls. Differentially accessible ATAC-seq peaks with an adjusted p-value ≤ 0.05 are indicated by bars below significant peaks. Navy bars indicate significantly decreased accessibility relative to AAVS1 KO controls; red bars indicate significantly increased accessibility (Padj ≤ 0.05; n = 2 donors x 1 gRNA for KO and 7-8 gRNA targeting AAVS1).

Supplementary Figure Legends

Figure S1. CRISPRi *FOXP3* locus tiling screen identifies cis-regulators of FOXP3 in Tconv.
a. Flow cytometry plots depicting FOXP3 and HELIOS expression in CRISPRi tiling screen Treg and Tconv donors 7 days post-initial stimulation. **b.** Representative flow cytometry plots of FOXP3 expression in AAVS1-targeted Tconvs at 0, 24, and 48 hours post-restimulation with anti-CD28/CD3/CD2 antibody complexes. **c.** Example representative gating strategy of Tconvs (top) and Tregs (bottom) FOXP3 expression in CRISPRi tiling screen. **d.** CRISPRi *FOXP3* locus-tiling screen log2 fold change gRNA enrichment in FOXP3 low vs. high FACS bins in individual Treg and Tconv donors, plotted along the *FOXP3* locus. Neighboring gRNAs were grouped into sliding 500 bp bins, shifted 50 bp at a time, for analyses, and individual points indicate grouped bins. *Blue*, gRNA bin enriched in FOXP3 High FACS bin. *Red*, gRNA bin enriched in FOXP3 Low FACS bin. *Outlined*, FDR less than or equal to 0.05. Tconv Donor 2 showed no low bin enrichment at the positive control *FOXP3* TSS and was subsequently excluded from the combined donor analysis. **e.** ATAC-seq in unstimulated (dark gray) and stimulated (light gray) Tconv and Treg[22]. Positive cis-elements CNS0, the *FOXP3* TSS, and TcNS+ are highlighted in red. Negative cis-element TcNS- is highlighted in blue.

Figure S2. CRISPRn screen identifies Tconv FOXP3 trans-regulators.
a. Example representative gating strategy of Tconv FOXP3 expression in CRISPRn trans-regulator screen. **b.** Number of sorted cells per gRNA in the library in FOXP3 low and high FACS bins across three donors. **c-e.** CRISPRn trans-regulator screen donor correlation plots of log2 fold change of gene gRNA enrichment in FOXP3 high vs. low FACS bins. Color of points indicates significance. *Pink*, significant in both donors. *Blue/green*, significant in indicated donor only. *Gray*, not significant (FDR ≤ 0.05).

Figure S3. CRISPRn screen arrayed validation characterizes Tconv FOXP3 trans-regulators.
a-b. Representative gating strategy of Tconv %FOXP3+ cells in arrayed validation at 0 hours post-stimulation (a) and 48 hours post-stimulation (b). FOXP3+ gate was set on cells receiving a FOXP3 KO gRNA, as shown. **c.** Arrayed validation of top FOXP3 maintenance and suppressive regulators in Tconv at 0 and 48 hours post-stimulation. Color indicates directional effect in screen. FOXP3 MFI in each targeted sample is normalized to the donor-matched mean of AAVS1-targeting controls (n = 2 donors x 2 gRNAs per target or 6 gRNAs targeting AAVS1 control). **d.** Editing efficiency (% modified reads) of arrayed validation genes and AAVS1-targeting controls. Color of bars indicates individual gRNAs (n = 2 donors x 2 gRNA per gene or 6 gRNA targeting AAVS1 control). **e.** Arrayed validation of top Tconv FOXP3 maintenance and suppressive regulators in Tregs at 0 and 48 hours post-stimulation. Color indicates directional effect in Tconv screen. FOXP3 MFI for each targeted sample is normalized to the donor-matched mean of AAVS1-targeting controls (n = 2 donors x 2 gRNAs per target or 6 gRNAs targeting AAVS1 control).

Figure S4. Interaction of FOXP3 trans-regulators with the FOXP3 locus and other trans-regulators.
a. Effect of regulator KO on expression[24] of CRISPRi-tiled *FOXP3* locus genes. Colored tiles indicate significant differential expression. Genes without significant differential expression across all samples are excluded. *Light blue*, negative regulator in Tconv screen. *Red*, positive

regulator in Tconv screen (*Padj* ≤ 0.05). **b.** Effect of regulator KO on expression[24] of FOXP3 trans-regulators. Colored tiles indicate significant differential expression. Genes without significant differential expression across all samples are excluded. *Light blue*, negative regulator in Tconv screen. *Red*, positive regulator in Tconv screen (*Padj* ≤ 0.05).

Supplementary Tables

S1. CRISPRi gRNA library.
S2. CRISPRi screen gRNA counts generated with MAGeCK.
S3. CRISPRi screen Treg results generated with DESeq2.
S4. CRISPRi screen Tconv results generated with DESeq2.
S5. CRISPRn screen gRNA counts generated with MAGeCK.
S6. CRISPRn screen gene-level results generated with MAGeCK.
S7. CRISPRn screen gRNA-level results generated with MAGeCK.
S8. List of gRNAs used in arrayed experiments.

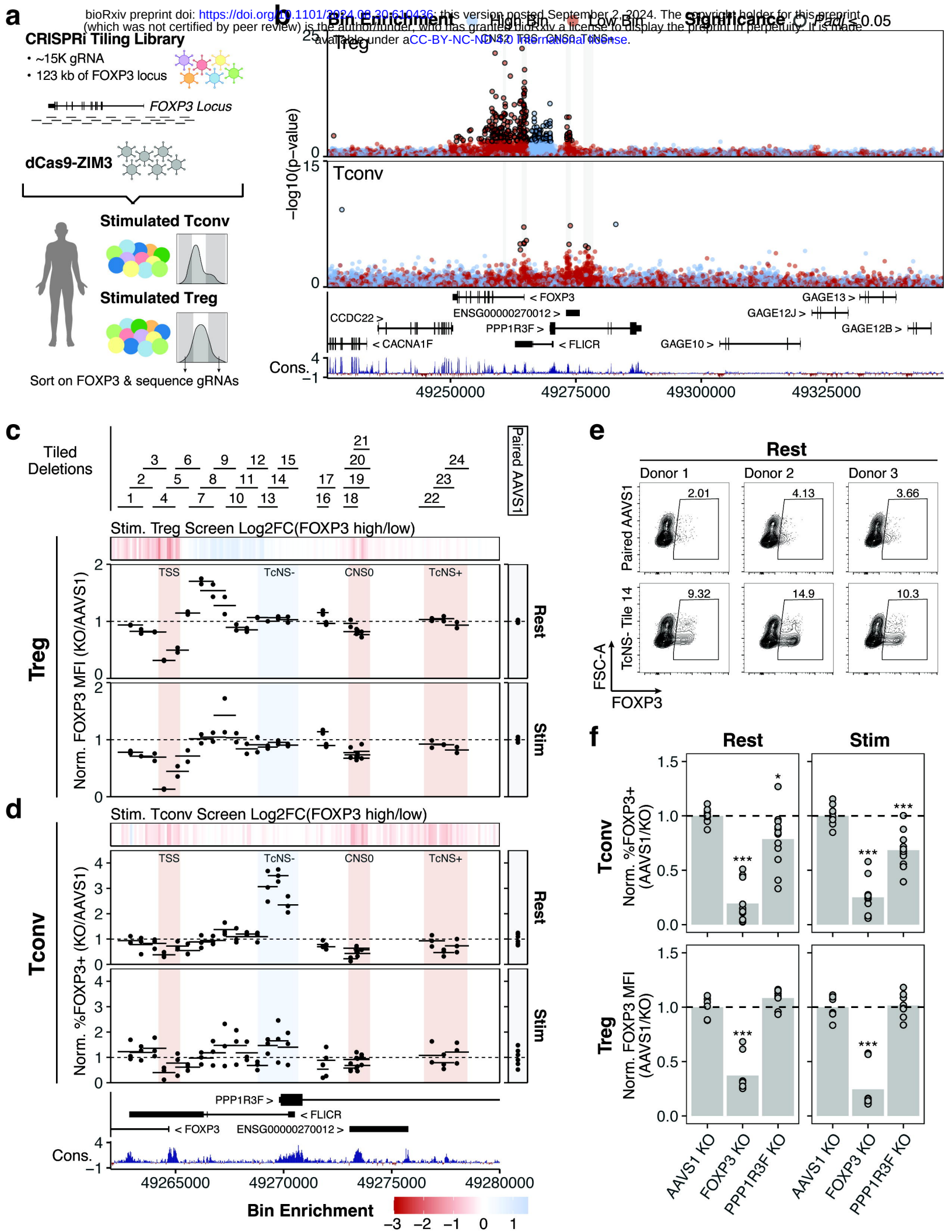

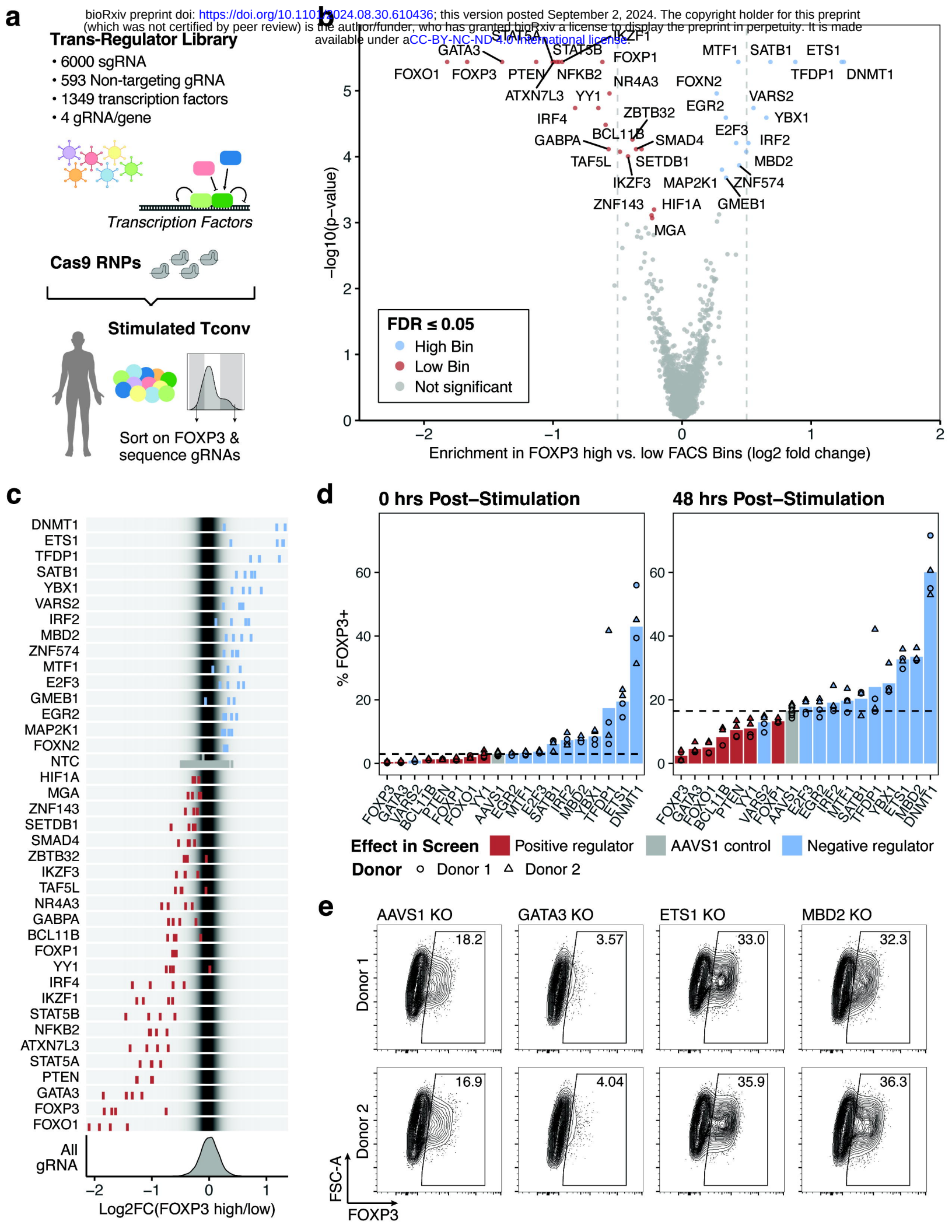

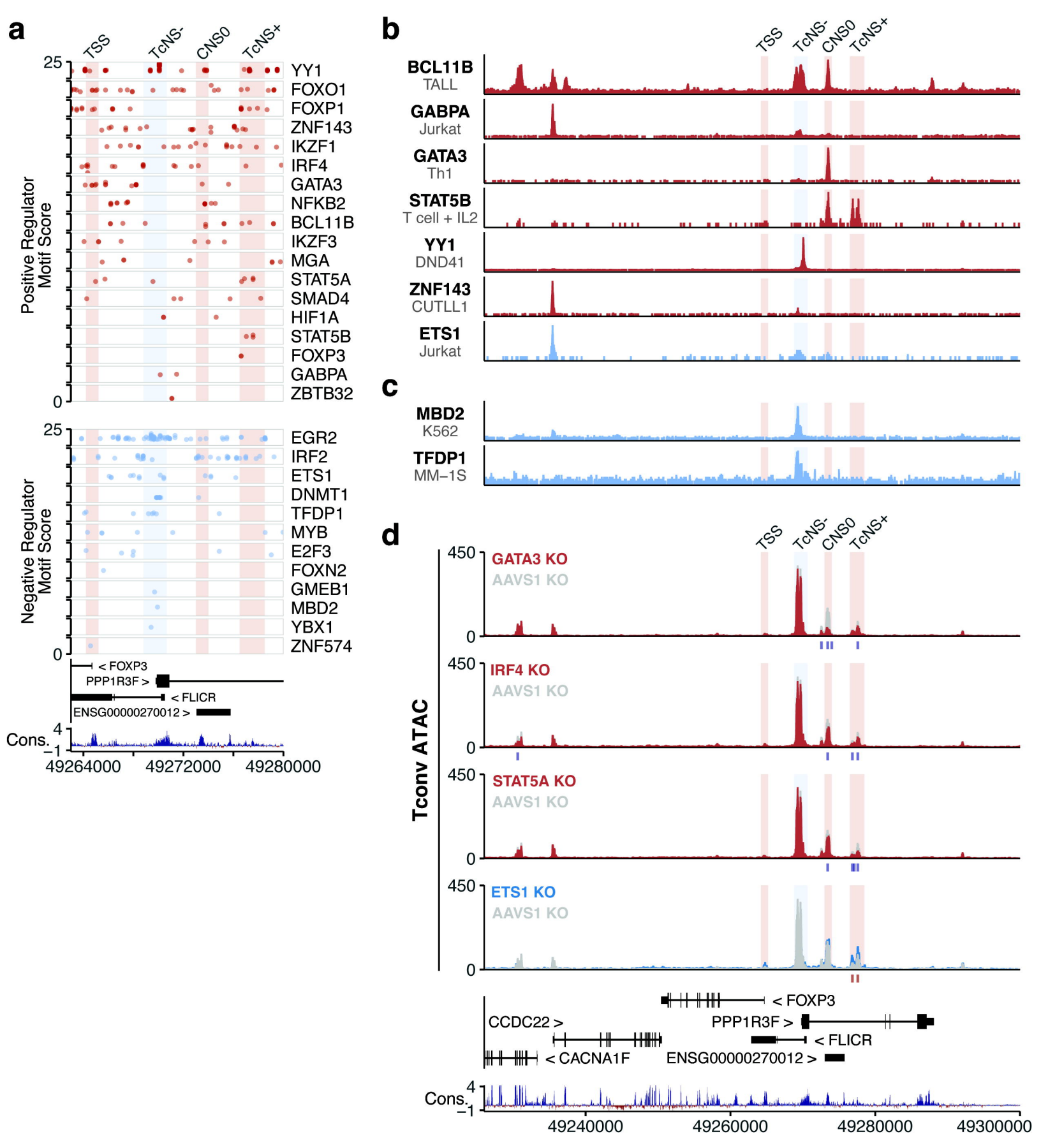
a
TSS
TcNS-
CNS0
TcNS+
Positive Regulator Motif Score
25
0
YY1
FOXO1
FOXP1
ZNF143
IKZF1
IRF4
GATA3
NFKB2
BCL11B
IKZF3
MGA
STAT5A
SMAD4
HIF1A
STAT5B
FOXP3
GABPA
ZBTB32
Negative Regulator Motif Score
25
0
EGR2
IRF2
ETS1
DNMT1
TFDP1
MYB
E2F3
FOXN2
GMEB1
MBD2
YBX1
ZNF574
< FOXP3
PPP1R3F >
< FLICR
ENSG00000270012 >
Cons.
4
−1
49264000
49272000
49280000
b
TSS
TcNS-
CNS0
TcNS+
BCL11B
TALL
GABPA
Jurkat
GATA3
Th1
STAT5B
T cell + IL2
YY1
DND41
ZNF143
CUTLL1
ETS1
Jurkat
c
MBD2
K562
TFDP1
MM−1S
d
TSS
TcNS-
CNS0
TcNS+
Tconv ATAC
450
0
GATA3 KO
AAVS1 KO
IRF4 KO
AAVS1 KO
STAT5A KO
AAVS1 KO
ETS1 KO
AAVS1 KO
< FOXP3
CCDC22 >
PPP1R3F >
< FLICR
< CACNA1F
ENSG00000270012 >
Cons.
4
−1
49240000
49260000
49280000
49300000

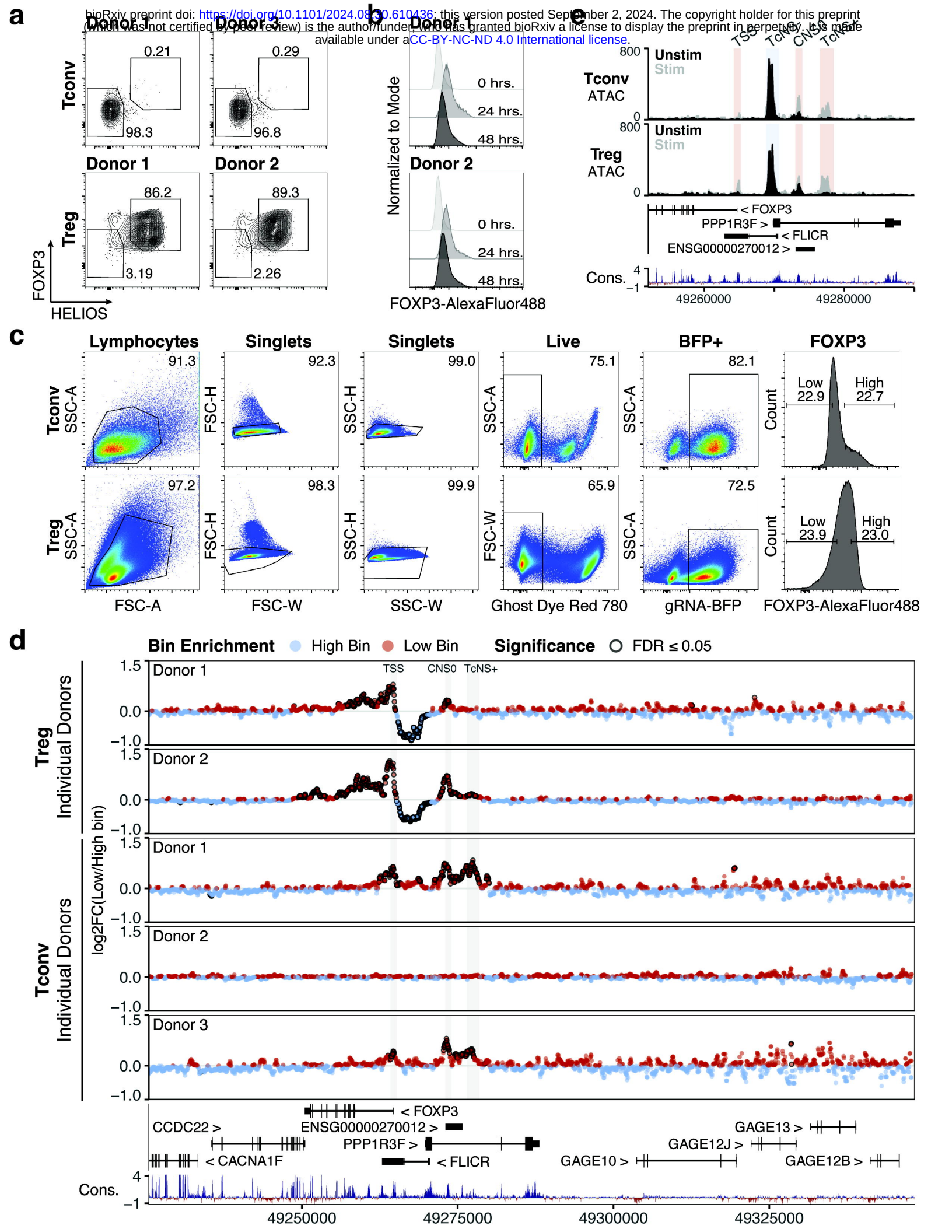

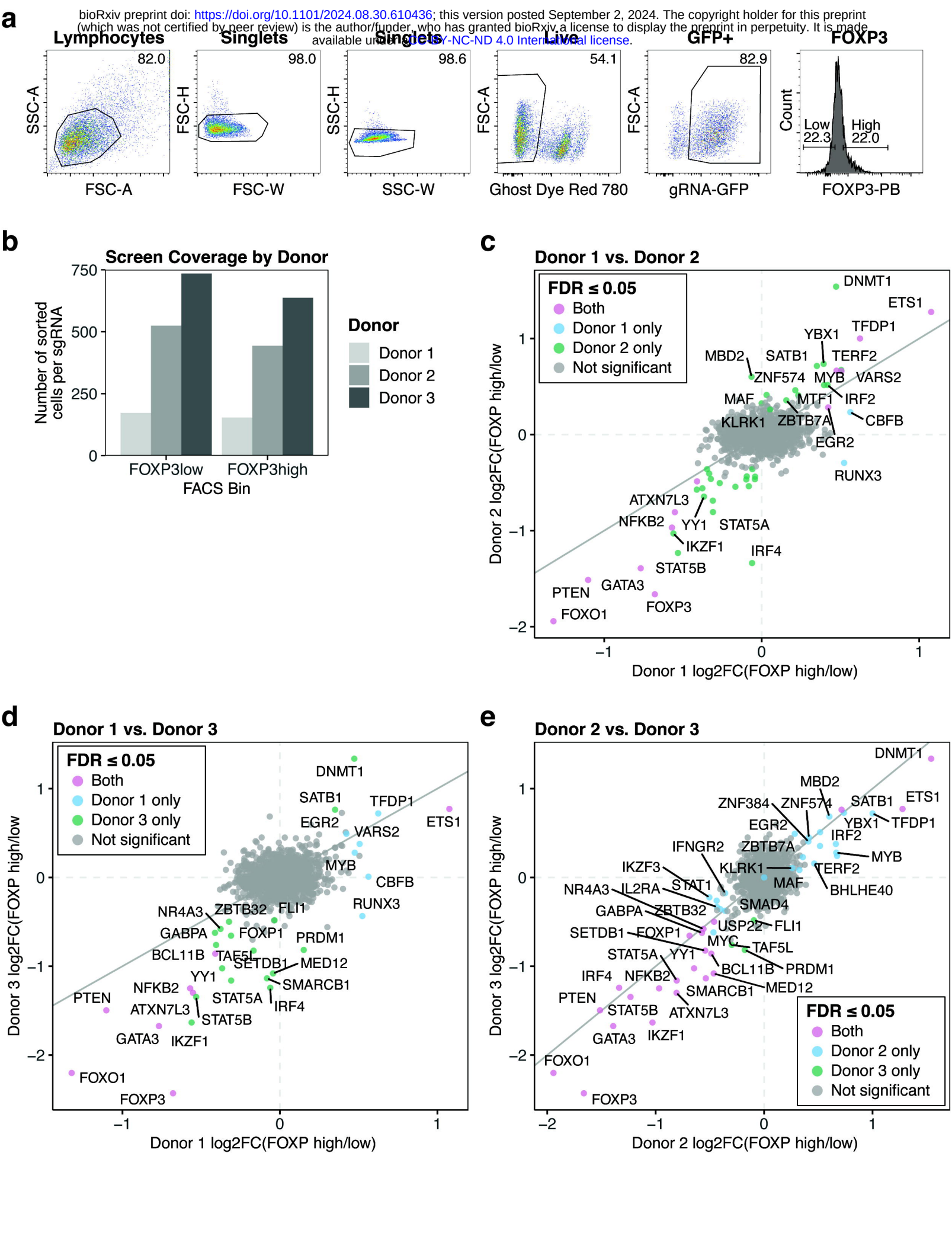

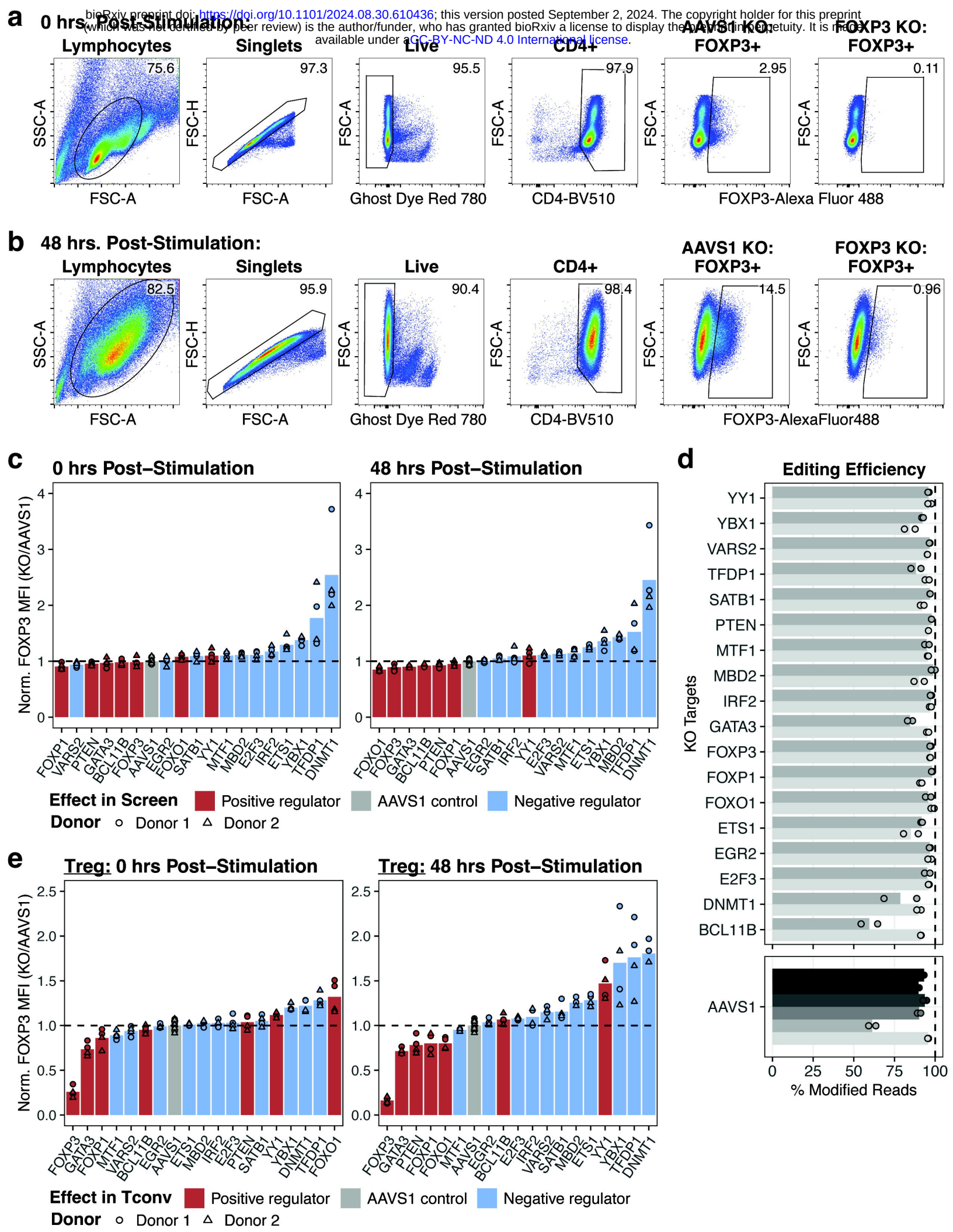

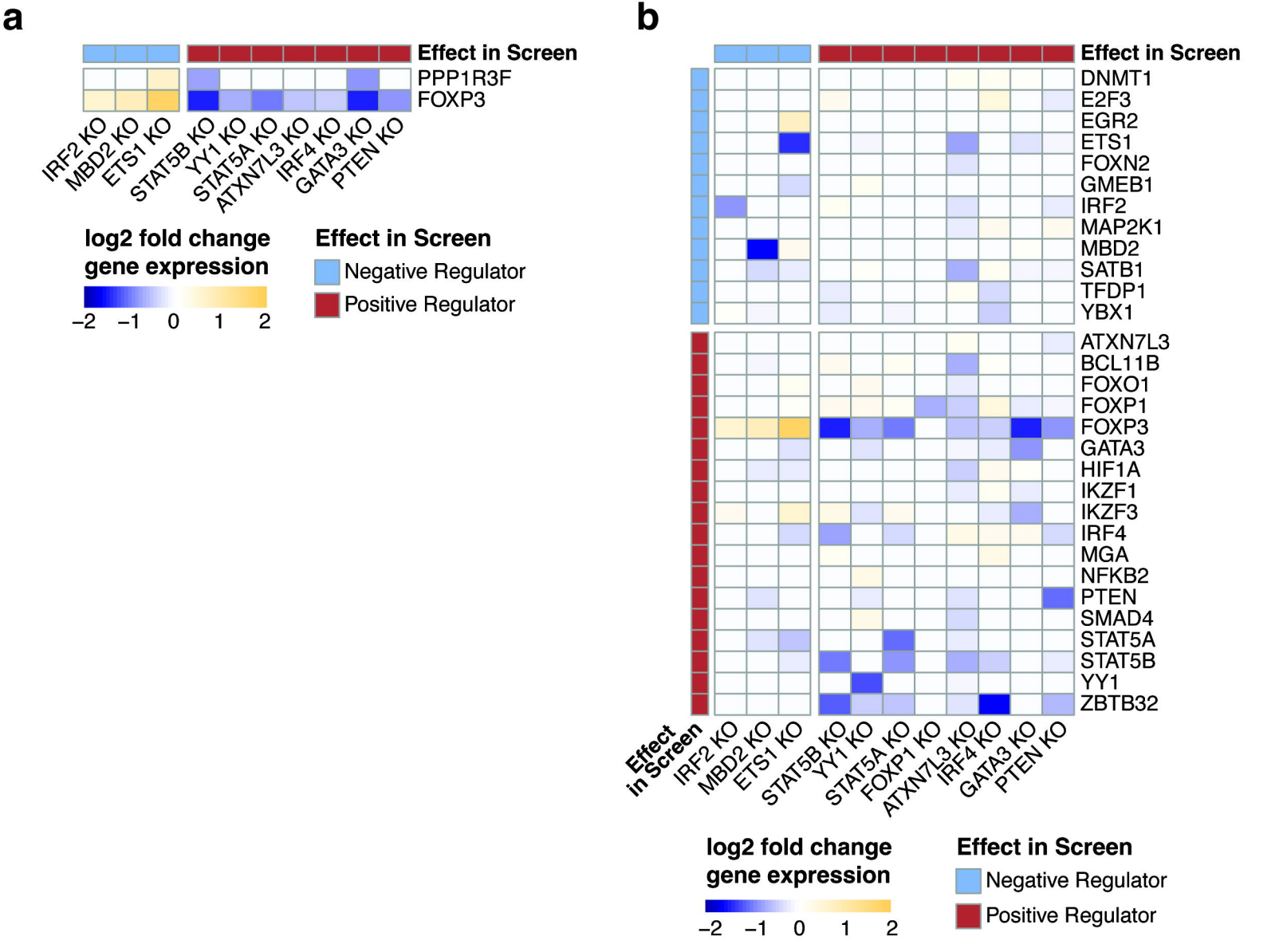
a
Effect in Screen
PPP1R3F
FOXP3
IRF2 KO
MBD2 KO
ETS1 KO
STAT5B KO
YY1 KO
STAT5A KO
ATXN7L3 KO
IRF4 KO
GATA3 KO
PTEN KO
log2 fold change gene expression
−2 −1 0 1 2
Effect in Screen
Negative Regulator
Positive Regulator
b
Effect in Screen
DNMT1
E2F3
EGR2
ETS1
FOXN2
GMEB1
IRF2
MAP2K1
MBD2
SATB1
TFDP1
YBX1
ATXN7L3
BCL11B
FOXO1
FOXP1
FOXP3
GATA3
HIF1A
IKZF1
IKZF3
IRF4
MGA
NFKB2
PTEN
SMAD4
STAT5A
STAT5B
YY1
ZBTB32
Effect in Screen
IRF2 KO
MBD2 KO
ETS1 KO
STAT5B KO
YY1 KO
STAT5A KO
FOXP1 KO
ATXN7L3 KO
IRF4 KO
GATA3 KO
PTEN KO
log2 fold change gene expression
−2 −1 0 1 2
Effect in Screen
Negative Regulator
Positive Regulator